NATIONAL ADVISORY COMMITTEE
FOR AERONAUTICS

REPORT No. 601

TORSION TESTS OF TUBES

By AMBROSE H. STANG, WALTER RAMBERG, and GOLDIE BACK

1937

AERONAUTIC SYMBOLS

1. FUNDAMENTAL AND DERIVED UNITS

	Symbol	Metric		English	
		Unit	Abbreviation	Unit	Abbreviation
Length_____	l	meter_____	m	foot (or mile)_____	ft. (or mi.)
Time_____	t	second_____	s	second (or hour)_____	sec. (or hr.)
Force_____	F	weight of 1 kilogram_____	kg	weight of 1 pound_____	lb.
Power_____	P	horsepower (metric)_____	_____	horsepower_____	hp.
Speed_____	V	{kilometers per hour_____	k.p.h.	miles per hour_____	m.p.h.
		{meters per second_____	m.p.s.	feet per second_____	f.p.s.

2. GENERAL SYMBOLS

W,   Weight$=mg$

g,   Standard acceleration of gravity$=9.80665$ m/s^2 or 32.1740 ft./sec.^{2}

m,   Mass$=\dfrac{W}{g}$

I,   Moment of inertia$=mk^2$. (Indicate axis of radius of gyration k by proper subscript.)

μ,   Coefficient of viscosity

ν,   Kinematic viscosity

ρ,   Density (mass per unit volume)

Standard density of dry air, 0.12497 kg-m^{-4}-s^2 at 15° C. and 760 mm; or 0.002378 lb.-ft.$^{-4}$ sec.^{2}

Specific weight of "standard" air, 1.2255 kg/m^3 or 0.07651 lb./cu. ft.

3. AERODYNAMIC SYMBOLS

S,   Area

S_w,   Area of wing

G,   Gap

b,   Span

c,   Chord

$\dfrac{b^2}{S}$,   Aspect ratio

V,   True air speed

q,   Dynamic pressure$=\dfrac{1}{2}\rho V^2$

L,   Lift, absolute coefficient $C_L=\dfrac{L}{qS}$

D,   Drag, absolute coefficient $C_D=\dfrac{D}{qS}$

D_0,   Profile drag, absolute coefficient $C_{D_0}=\dfrac{D_0}{qS}$

D_i,   Induced drag, absolute coefficient $C_{D_i}=\dfrac{D_i}{qS}$

D_p,   Parasite drag, absolute coefficient $C_{D_p}=\dfrac{D_p}{qS}$

C,   Cross-wind force, absolute coefficient $C_c=\dfrac{C}{qS}$

R,   Resultant force

i_w,   Angle of setting of wings (relative to thrust line)

i_t,   Angle of stabilizer setting (relative to thrust line)

Q,   Resultant moment

Ω,   Resultant angular velocity

$\rho\dfrac{Vl}{\mu}$,   Reynolds Number, where l is a linear dimension (e.g., for a model airfoil 3 in. chord, 100 m.p.h. normal pressure at 15° C., the corresponding number is 234,000; or for a model of 10 cm chord, 40 m.p.s., the corresponding number is 274,000)

C_p,   Center-of-pressure coefficient (ratio of distance of c.p. from leading edge to chord length)

α,   Angle of attack

ϵ,   Angle of downwash

α_0,   Angle of attack, infinite aspect ratio

α_i,   Angle of attack, induced

α_a,   Angle of attack, absolute (measured from zero-lift position)

γ,   Flight-path angle

REPORT No. 601

TORSION TESTS OF TUBES

By AMBROSE H. STANG, WALTER RAMBERG
and GOLDIE BACK

National Bureau of Standards

NATIONAL ADVISORY COMMITTEE FOR AERONAUTICS

HEADQUARTERS, NAVY BUILDING, WASHINGTON, D. C.

LABORATORIES, LANGLEY FIELD, VA.

Created by act of Congress approved March 3, 1915, for the supervision and direction of the scientific study of the problems of flight (U. S. Code, Title 50, Sec. 151). Its membership was increased to 15 by act approved March 2, 1929. The members are appointed by the President, and serve as such without compensation.

JOSEPH S. AMES, Ph. D., *Chairman*,
 Baltimore, Md.
DAVID W. TAYLOR, D. Eng., *Vice Chairman*,
 Washington, D. C.
WILLIS RAY GREGG, Sc. D., *Chairman, Executive Committee*,
 Chief, United States Weather Bureau.
CHARLES G. ABBOT, Sc. D.,
 Secretary, Smithsonian Institution.
LYMAN J. BRIGGS, Ph. D.,
 Director, National Bureau of Standards.
ARTHUR B. COOK, Rear Admiral, United States Navy,
 Chief, Bureau of Aeronautics, Navy Department.
FRED D. FAGG, JR., J. D.,
 Director of Air Commerce, Department of Commerce.
HARRY F. GUGGENHEIM, M. A.,
 Port Washington, Long Island, N. Y.

SYDNEY M. KRAUS, Captain, United States Navy,
 Bureau of Aeronautics, Navy Department.
CHARLES A. LINDBERGH, LL. D.,
 New York City.
WILLIAM P. MACCRACKEN, J. D.,
 Washington, D. C.
AUGUSTINE W. ROBINS, Brigadier General, United States Army,
 Chief Matériel Division, Air Corps, Wright Field, Dayton, Ohio.
EDWARD P. WARNER, M. S.,
 Greenwich, Conn.
OSCAR WESTOVER, Major General, United States Army,
 Chief of Air Corps, War Department.
ORVILLE WRIGHT, Sc. D.,
 Dayton, Ohio.

GEORGE W. LEWIS, *Director of Aeronautical Research*

JOHN F. VICTORY, *Secretary*

HENRY J. E. REID, *Engineer in Charge, Langley Memorial Aeronautical Laboratory, Langley Field, Va.*

JOHN J. IDE, *Technical Assistant in Europe, Paris, France*

TECHNICAL COMMITTEES

AERODYNAMICS
POWER PLANTS FOR AIRCRAFT
AIRCRAFT MATERIALS

AIRCRAFT STRUCTURES
AIRCRAFT ACCIDENTS
INVENTIONS AND DESIGNS

Coordination of Research Needs of Military and Civil Aviation

Preparation of Research Programs

Allocation of Problems

Prevention of Duplication

Consideration of Inventions

LANGLEY MEMORIAL AERONAUTICAL LABORATORY

LANGLEY FIELD, VA.

Unified conduct, for all agencies, of scientific research on the fundamental problems of flight.

OFFICE OF AERONAUTICAL INTELLIGENCE

WASHINGTON, D. C.

Collection, classification, compilation, and dissemination of scientific and technical information on aeronautics.

REPORT No. 601

TORSION TESTS OF TUBES

By Ambrose H. Stang, Walter Ramberg, and Goldie Back

SUMMARY

Torsion tests of 63 chromium-molybdenum steel tubes and 102 17ST aluminum-alloy tubes of various sizes and lengths were made to study the dependence of the torsional strength on both the dimensions of the tube and the physical properties of the tube material. Three types of failure were found to be important for sizes of tubes frequently used in aircraft construction: (1) failure by plastic shear, in which the tube material reached its yield strength before the critical torque was reached; (2) failure by elastic two-lobe buckling, which depended only on the elastic properties of the tube material and the dimensions of the tube; and (3) failure by a combination of (1) and (2), that is, by buckling taking place after some yielding of the tube material.

An adequate theory exists for explaining failure by (1) or (2). Most of the tubes failed by the combined failure (3), for which a theoretical solution seems unattainable at this time. An analysis of the data showed that the torsional strength of these tubes could be expressed by an empirical formula involving only the tensile properties of the tube material in addition to the dimensions of the tube. Design charts were computed from this empirical formula and a number of examples were worked out to facilitate the application of the charts.

INTRODUCTION

Thin-wall tubes are commonly used in airplanes to transmit torques to the ailerons and other control surfaces. It is well known that the maximum fiber stress in torsion that a thin-wall tube will support depends on the ratio (t/D) of its wall thickness to its diameter. Tests have been made (references 1, 2, 3, and 4) to determine the relationship between torsional strength and t/D ratio for tubes of various materials, but the available data resulting from these tests were insufficient to lead to general conclusions or even to determine a fairly accurate design formula for a given material.

It seemed desirable, therefore, to carry out a series of tests with a sufficiently large number of tubes of various lengths and t/D ratios and, if possible, of several materials to supply such data. The present report describes the results of torsion tests of 63 chromium-molybdenum steel tubes and 102 tubes of 17ST aluminum alloy. These tests were made at the National Bureau of Standards with the cooperation of the Bureau of Aeronautics, Navy Department, and the National Advisory Committee for Aeronautics.

APPARATUS AND TESTS

TUBES

The lengths L of the steel tubes ranged from 19 to 60 inches, outside diameters D from ¾ to 2½ inches, thicknesses t from 0.03 to 0.125 inch, t/D ratios from 0.0134 to 0.0840, and L/D ratios from 7.6 to 80.0. The aluminum-alloy tubes were cut in lengths of 20 and 60 inches; their outside diameters ranged from 1 to 2 inches, their wall thicknesses from 0.019 to 0.221 inch, their t/D ratios from 0.0101 to 0.1192, and L/D ratios from 10.0 to 60.2.

The first five lengths (A_o, B_o, C_o, D_o, E_o) of chromium-molybdenum steel tubes used in the tests were purchased under Army Specification 57–180–2A; the other tubes (F_o to V_o) were bought under Navy Department Specification 44T18. Table I shows that the tensile properties required by these specifications are the same. Somewhat higher properties are required by the more recent Navy Department Specification 44T18a, which is included in table I for the sake of completeness.

TABLE I.—MECHANICAL SPECIFICATION FOR CHROMIUM-MOLYBDENUM STEEL TUBES

Specification	Tensile strength (minimum) (lb./sq. in.)	Yield strength (minimum) (offset 0.2 percent) (lb./sq. in.)	Elongation in 2 inches (minimum) (percent)
Army 57–180–2A	95,000	60,000	10
Navy 44T18	95,000	60,000	10
Navy 44T18a	95,000	75,000	10

The aluminum-alloy tubes were contributed by the Aluminum Company of America. They were manufactured to satisfy Navy Department Specification 44T21. The mechanical properties listed in this specification are given in table II.

1

TABLE II.—MECHANICAL SPECIFICATION FOR HEAT-TREATED ALUMINUM-ALLOY TUBES

Specification	Nominal outside diameter (in.)	Tensile strength (minimum) (lb./sq. in.)	Yield strength (minimum) (offset 0.2 percent) (lb./sq. in.)	Elongation in 2 inches (minimum) (percent)
Navy 44T21	¼ to 1	55,000	40,000	16
	Over 1 to 1½	55,000	40,000	14
	Over 1½ to 4	55,000	40,000	12

The chemical composition of a few of the steel tubes was determined and the Vickers hardness numbers and tensile properties of each length of tube were obtained before carrying out the torsion tests.

Table III gives the results of analyses made by the Chemistry Division of the National Bureau of Standards on five of the steel tubes selected at random.

TABLE III.—PERCENTAGE OF CHEMICAL ELEMENTS PRESENT IN CHROMIUM-MOLYBDENUM STEEL TUBES

Specimen	Carbon	Manganese	Phosphorus	Sulphur	Chromium	Molybdenum
D	0.34	0.54	0.022	0.011	1.09	0.19
K	.30	.49	.022	.009	.86	.18
N	.31	.59	.029	.013	1.11	.24
O	.39	.49	.021	.013	.86	.23
S	.32	.53	.023	.015	.97	.23

No such analyses were made of the aluminum-alloy tubes, but the nominal composition furnished by the manufacturer is given in table IV.

TABLE IV.—NOMINAL CHEMICAL COMPOSITION OF 17ST TUBES AS GIVEN BY MANUFACTURER, PERCENTAGE

Copper _____ 4.0
Manganese _____ .5
Magnesium _____ .5
Aluminum _____ 95.0

Vickers hardness tests were made at both ends of each tube. The results for the chromium-molybdenum steel tubes are given in table V and those for the aluminum-alloy tubes in table VI. For the steel tubes the Vickers numbers varied from 204 to 311. The average variation for a single tube was less than 5 percent and in only one case (tube O_o, 13.2 percent) did it exceed 10 percent. The Vickers numbers for the aluminum-alloy tubes varied from 125 to 142, the maximum variation for a single tube being less than 2½ percent.

The dimensions of the chromium-molybdenum steel specimens used in the torsion tests are included in table VII and those of the 17ST aluminum-alloy specimens, in table VIII, together with data obtained from the torsion tests.

TENSILE TESTS

Tensile tests were made on specimens 19 to 20 inches long cut from each length of tubing. The specimens were fitted with plugs similar to those described in Navy Department specification 44T18 and were held in V-type jaws attached to the two heads of the testing machine. A hydraulic machine of 100,000-pound capacity was used to test all except one of the chromium-molybdenum steel tubes; this one specimen was tested in a machine of the lever type because its diameter of 2½ inches was too large for the jaws provided with the hydraulic machine. All the aluminum-alloy tensile specimens were tested in lever-type machines of 2,000-, 50,000-, and 100,000-pound capacity. All of the steel specimens except A_o, D_o, and $E_{\bullet}$ were prestressed in tension to about 30,000 pounds per square inch. The prestressing served to seat the strain gages and to cold-work the material sufficiently in the low-stress range to obtain from it an approximately straight stress-strain curve, from which the Young's modulus of the material could be derived. The aluminum-alloy tubes had already been prestressed at the factory and only enough load was put on the specimen before test to seat the strain gages securely.

Tensile strains on the steel tubes were measured with a Ewing extensometer using a 2-inch gage length (smallest scale division 0.0001 in./in.) for specimens 1½ inches in diameter or less, and with a Huggenberger extensometer using a 1-inch gage length (smallest scale division 0.00015 in./in.) for tubes of larger diameter. Tuckerman optical strain gages with a 2-inch gage length were used for all aluminum-alloy tubes. The smallest scale division on the vernier of this gage corresponds to a strain increment of 0.000002 in./in.

The strain gages on each of the tensile specimens were placed 8 to 9 inches, or 4 to 9 diameters, away from the jaws gripping both ends of the specimen. A study of the stress distribution in a $2.5 \times 0.032 \times 36$ inch tube of chromium-molybdenum steel held between V-type jaws making contact at opposite pairs of points 60° apart had shown that the average of the strains at two ends of any diameter in a cross section removed 3 diameters or more from the ends gave the same value within the error of observation. At a cross section 1½ diameters from any pair of jaws the average strains varied ±6 percent about an average stress of 15,000 pounds per square inch and through ±2.6 percent about an average stress of 27,000 pounds per square inch. From these observations it was concluded that the average strains as measured in the present series of specimens from 4 to 9 diameters from the jaws were correct within the error of observation. The contact points of the jaws in these specimens were more than 60° apart except for some of the 1-inch tubes for which they were a little closer; in the latter case, however, the gages were about 8 diameters away from the jaws.

From each stress-strain curve the yield strength was determined as the stress at which the strain was 0.002 in./in. in excess of the elastic strain with an assumed Young's modulus of 30×10^6 pounds per square inch for the chromium-molybdenum steel tubes and a modulus of 10×10^6 pounds per square inch for the aluminum-alloy tubes. The values are given in table V for the steel tubes and in table VI for the aluminum-alloy tubes. It is seen that the yield strength of the steel

tubes varied from 67,700 to 110,000 and that of the aluminum-alloy tubes, from 44,300 to 50,000 pounds per square inch.

Young's modulus E was obtained by plotting against stress σ the difference $\Delta\epsilon$ between the observed strain and that computed from an assumed modulus E_0 of 30×10^6 pounds per square inch in the case of the steel tubes and a modulus of 10×10^6 pounds per square inch in the case of the aluminum-alloy tubes and by measuring the slope $\Delta\epsilon/\sigma$ of the straight line giving the best fit to the plotted points. The true modulus E is then computed from this slope using the simple relation

$$\frac{1}{E}=\frac{1}{E_o}+\frac{\Delta\epsilon}{\sigma} \tag{1}$$

Tables V and VI show that the Young's modulus for

Examination of the stress-strain curves for the steel specimens showed that the material could be divided into two groups with markedly different stress-strain curves. For the greater number of steel tubes the curves were nearly straight until near the yield stress, where they bent fairly sharply. In these specimens the ratio of tensile strength to yield strength varied from 1.03 to about 1.18. Three of these curves (for specimens H_0, R_0, K_0) are shown in figure 1a. For other specimens, however, the slope of the curves decreased gradually with no sharp bend. For these specimens the ratio of tensile strength to yield strength was much higher, ranging from 1.37 to 1.63. Figure 1a also gives three of these curves (for specimens I_0, V_0, N_0). In each of these groups there existed a rough association between different tensile properties. Low tensile
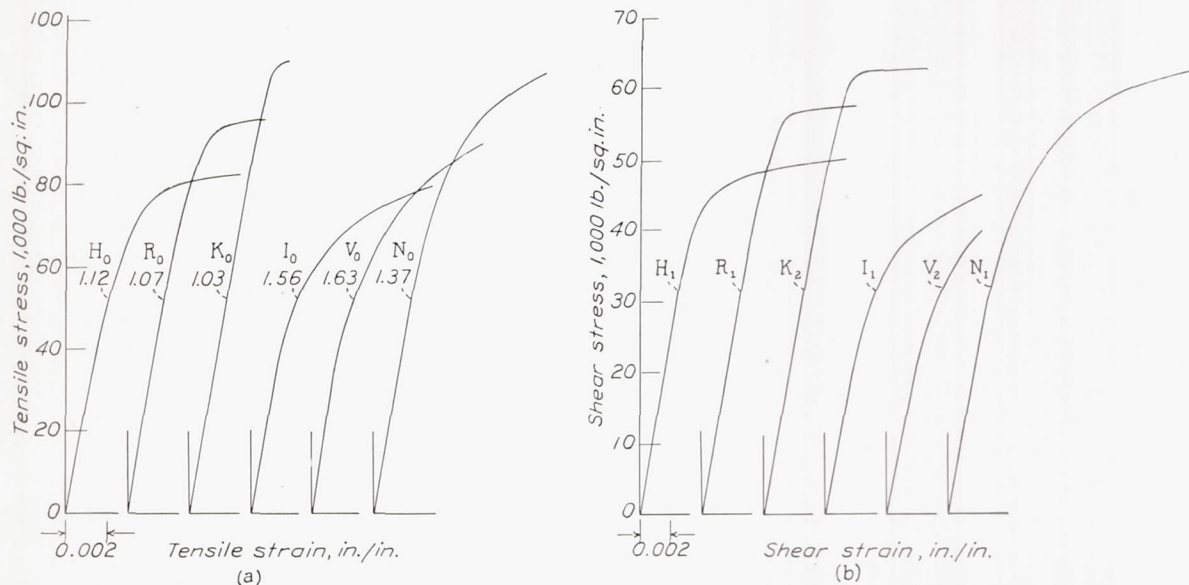

FIGURE 1.—Stress-strain curves of chromium-molybdenum steel tubes. Tensile specimens H_0, R_0, K_0, with sharp knee near the yield strength were cut from the same three lengths of tubing as shear specimens H_1, R_1, K_2, respectively; similarly tensile specimens, I_0, V_0, N_0, with relatively rounded knee near the yield strength, were cut from the same three lengths as shear specimens I_1, V_2, N_1, respectively. The ratio of tensile strength to yield strength in tension is shown as a number on each tensile stress-strain curve.

the steel tubes ranged from 27.3 to 30.2×10^6 pounds per square inch and that for the aluminum-alloy tubes varied from 9.79 to 10.81×10^6 pounds per square inch. In both groups the range of variation was close to 10 percent.

Elongations over a 2-inch gage length were determined by means of dividers; they varied from 11.5 to 32 percent for the steel tubes (table V) and from 17 to 34 percent for the aluminum-alloy tubes (table VI). The specimens that broke at the jaws were not considered in obtaining these limits.

Tables V and VI also give the tensile strength of each specimen. This value ranged from 88,400 to 132,900 pounds per square inch for the steel tubes and from 62,800 to 67,000 pounds per square inch for the aluminum-alloy tubes.

strength, high yield strength, low elongation, low ratio of tensile strength to yield strength tend to occur together and high tensile strength is associated with low yield strength, high elongation, etc. However, no quantitative relation could be found between the results for materials in the two groups.

Not nearly so marked a differentiation into two groups was apparent for the aluminum-alloy tubes. The ratio of tensile strength to yield strength varied through a much smaller range, namely, from 1.27 to 1.49. Figure 2a shows three specimens with a relatively sharp knee near the yield stress (P_0, J_0, M_0) and three with a relatively rounded knee (U_0, s_0, x_0). There was again a rough tendency for low tensile strength to occur together with high yield strength, low elongation and low ratio of tensile strength to yield strength.
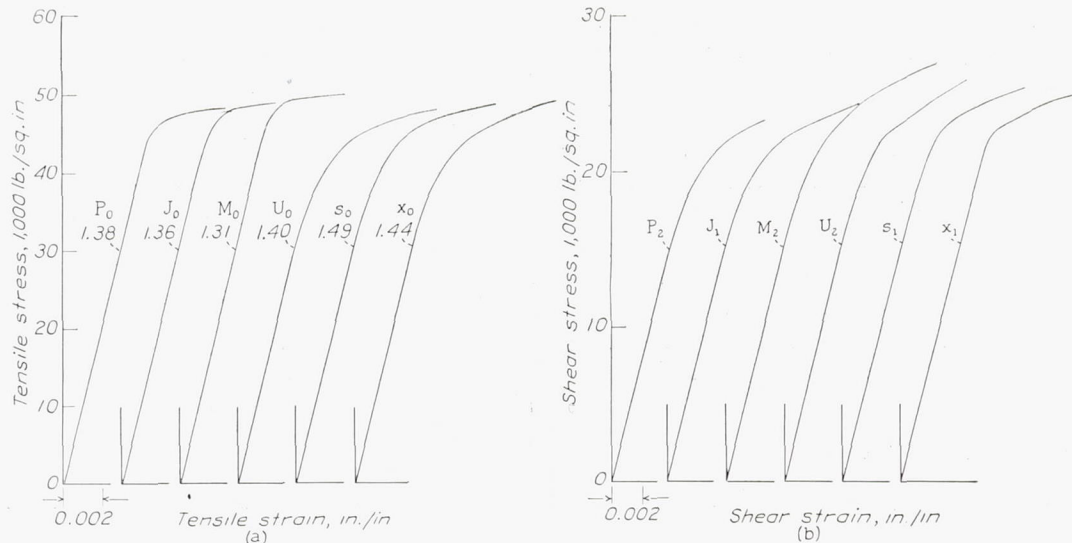
FIGURE 2.—Stress-strain curves of 17ST aluminum-alloy tubes. Tensile specimens P_0, J_0, M_0, with relatively sharp knee near the yield strength were cut from the same three lengths of tubing as shear specimens P_2, J_1, M_2, respectively; similarly tensile specimens U_0, s_0, x_0, with relatively rounded knee near the yield strength were cut from the same three lengths as shear specimens U_2, s_1, x_1, respectively. The ratio of tensile strength to yield strength in tension is shown as a number on each tensile stress-strain curve.

TORSION TESTS

Figure 3 shows the method of mounting the specimen for test in the torsion machine. The ends of the tube were reinforced by two steel plugs of proper diameter and were then clamped solidly between wedge-shaped jaws A; they were free to move in an axial direction throughout the test. Specimens not over 20 inches in length were tested in the 13,000 pound-inch pendulum-type machine shown in figure 3 and the longer tubes were tested in a 60,000 pound-inch lever-type machine.

The method of measuring the angle of twist under load is also shown in figure 3. The fixture consists of two rings B fastened to the specimen at points 25
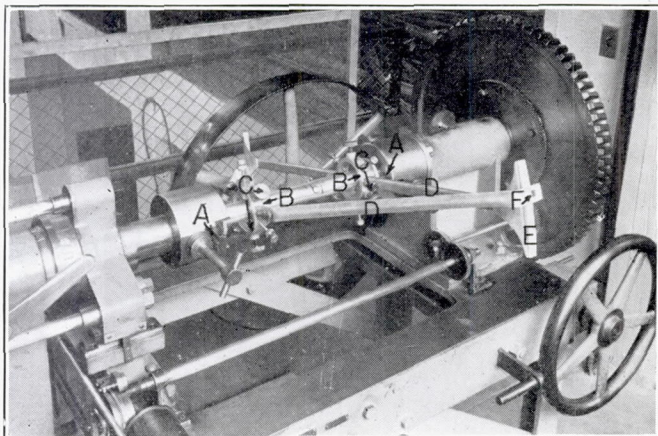

FIGURE 3.—Torsion testing machine with 17ST aluminum-alloy tube in position after test to failure.

centimeters (9.84 inches) apart by three screws C. Each ring carries a pair of aluminum radial arms D, one pair carrying the scales E and the other the pointers F. Readings were taken on both scales and averages were used to compensate for any effect due to bending of the tube under load.

CALCULATION OF SHEAR STRESSES

The torsion tests give the relation between the torque M transmitted by the tube and the angle of twist per unit length θ produced by that torque. The stress-strain curves in shear were computed from these torque-twist curves in the following manner.

The relation between the shear stress τ and the torque M in a twisted circular tube is given by the equation:

$$M(\theta) = 2\pi \int_{r_1}^{r_2} \tau r^2 dr \qquad (2)$$

where r is the radial distance from the axis of the tube

    r_1, radius of the inner wall.

    r_2, radius of the outer wall.

    τ, shear stress at a distance r from the axis.

The relation between this shear stress and the shear strain $\gamma = r\theta$,

$$\tau = f(\gamma) = f(r\theta) \qquad (3)$$

may be found by substituting (3) in (2) and differentiating both sides with respect to θ. (See reference 5, p. 128.) This gives the differential equation:

$$r_2^3 f(r_2\theta) - r_1^3 f(r_1\theta) = \frac{1}{2\pi}\left(\theta\frac{dM}{d\theta} + 3M\right) \qquad (4)$$

where $r_2\theta$, $r_1\theta$ are the shear strains at the outside and the inside wall of the tube, respectively. All quantities in this equation are given by the dimensions of the tube and the torque-twist curve except the stresses $f(r_2\theta)$ and $f(r_1\theta)$. The stress $f(r_2\theta)$ can, therefore, be calculated from equation (4) provided $f(r_1\theta)$ is known; this suggests a method of step-by-step solution beginning with the end of the elastic range in which $f(r_1\theta)$ is known. Practically, this method of computation is laborious and is not warranted by the accuracy of the data for tubes as thin as those tested in the present

investigation. It is entirely sufficient in these cases to use approximate methods based upon arbitrary simplifying assumptions.

A number of such methods have been used, all of them serving the purpose equally well. For this investigation the method chosen was to calculate the stress and strain in the mean fiber:

$$\bar{r} = \frac{1}{2}(r_1 + r_2) = \frac{D-t}{2}$$

on the assumption that both stresses and strains increase linearly with distance from the axis of the tube, as they do in the elastic case. This calculation gave

$$\tau = \frac{M\bar{r}}{I_p} = \frac{2M}{\pi D^2 t} \frac{1}{1 - 2\frac{t}{D} + 2\left(\frac{t}{D}\right)^2}$$
$$\gamma = \theta\bar{r} = \frac{\theta D}{2}\left(1 - \frac{t}{D}\right)$$
$$\tag{5}$$

where $D = 2r_2$ is the outside diameter of the tube and $t = r_2 - r_1$ is its wall thickness. Even for the thickest tubes tested $\left(\frac{t}{D} = 0.1192\right)$ the stresses so calculated could not differ by more than 14 percent from any stress existing in the wall. The stresses at the mean fiber calculated from (5) could not be in error by more than 1.5 percent for tubes up to $\frac{t}{D} = 0.12$. This value is the percentage difference in the mean fiber stress for a given twisting moment M calculated, on the one hand, by the extreme assumption of elastic twist corresponding to the first equation (5) and, on the other hand, by the extreme assumption of pure plastic shear (uniform shearing stress throughout).

Figures 1b and 2b show a number of stress-strain curves in shear derived from the moment-twist curve, with the help of (5).

The accuracy of the approximation (5) is brought out further by a comparison of exact and approximate analyses for a relatively thick $\left(\frac{t}{D} = 0.0562\right)$ steel tube and for one of the thickest aluminum-alloy tubes $\left(\frac{t}{D} = 0.1192\right)$. The exact and the approximate stress-strain curves for these two tubes are shown in figures 4 and 5. In each figure the two curves coincide within 1 percent for the most part and differ at no point by more than 2 percent. Their yield strengths in shear defined by the intersection of the sloping line with the stress-strain curve agree within a fraction of 1 percent.

The yield strengths obtained from the torsion tests with the help of equation (5) are listed in table VII for the steel tubes and in table VIII for the aluminum-alloy tubes.

Figure 6 shows four chromium-molybdenum steel tubes and four 17ST aluminum-alloy tubes after completion of the torsion test. The twist gages D (fig. 3)

were kept on the tubes until they failed either with a loud snap by two-lobe buckling (specimens P_1, B_1 fig. 6) or until the knee of the torque-twist curve had been well passed. In the latter case the torque increased slowly with increasing twist beyond the point at which the gages had been removed, until failure occurred either by gradual two-lobe buckling (Q_1, J_1), by helical
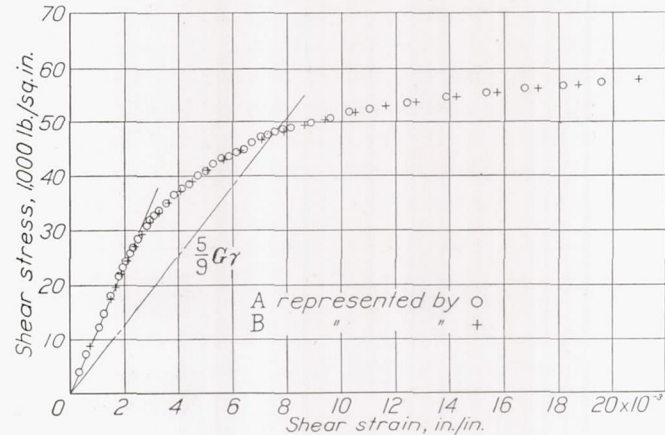

FIGURE 4.—Shear stress-strain curve for specimen J_1 (chromium-molybdenum, $t/D = 0.0562$) calculated from torque-twist curve.

A. Approximate method: Assume linear stress distribution across section as in elastic case, calculate stresses and strains at mean fiber from

$$\tau = \frac{2M}{\pi t D^2} \frac{1}{1 - 2\frac{t}{D} + 2\frac{t^2}{D^2}},$$

$$\gamma = \frac{\theta D}{2}\left(1 - \frac{t}{D}\right).$$

B. Exact method: Solve the recursion formula

$$\frac{\tau D\theta}{2} = \left(\frac{2}{D}\right)^3 \left\{\frac{1}{2\pi}\left[\theta\frac{dM}{d\theta} + 3M\right] + \left(\frac{D-2t}{2}\right)^3 \tau_{\left(\frac{D-2t}{2}\right)\theta}\right\}.$$

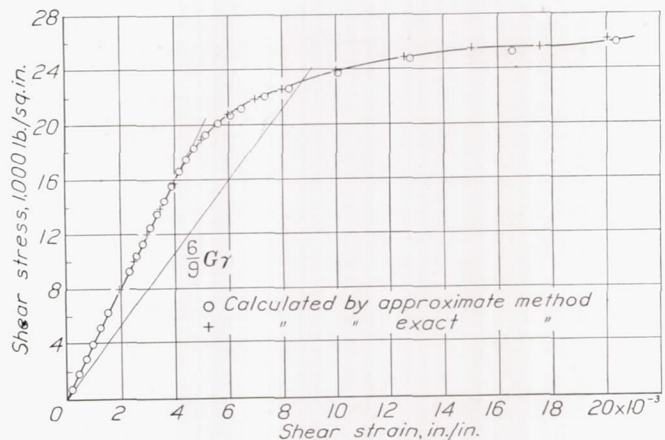FIGURE 5.—Shear stress-strain curve for specimen Aa_1 (17ST, $t/D = 0.1192$) calculated from torque-twist curve.

deformation of the axis of the tube (L_5, S_2) or, as in the case of some of the aluminum-alloy tubes, by a sudden fracture (T_1); specimen J_5 (fig. 6) would probably have failed by fracture if it had not developed a slight two-lobe buckle after twisting plastically through a large angle.

ANALYSIS OF RESULTS

DISCUSSION OF TYPES OF FAILURE

Observation of the failure of thin circular tubes in torsion has shown that three different limiting types of failure are of particular significance in engineering design:

1. Two-lobe buckling of the tube wall.
2. Helical deformation of the axis of the tube.
3. Plastic yielding of the material.

The first two types are caused by elastic instability of the twisted tube and do not necessarily involve permanent deformation of the material. They have been treated theoretically by Schwerin (reference 6).

Schwerin's formulas for the buckling strength of long tubes may be written in terms of the ratio t/D of wall thickness to outside diameter in the following form:

1. For two-lobe buckling

$$\tau = \frac{0.656E}{1-\mu^2}\left(\frac{t}{D}\right)^{3/2}\left(1+2.4\frac{t}{D}+\cdots\right) \quad (6)$$

where τ is the critical shear stress at the mean fiber; E, Young's modulus; and μ, Poisson's ratio of the material. Terms involving $\left(\frac{t}{D}\right)^2$ are neglected in the parentheses since they are small for tubes in which such elastic failure can take place.

2. For buckling of the axis of the tube into a helix Schwerin derived the formula

$$\tau = \frac{\pi E}{1-\mu}\frac{D}{L}\left(1-\frac{t}{D}+\frac{1}{3}\frac{t^2}{D^2}\cdots\right) \quad (7)$$

where L is the length of the tube.

3. If plastic yielding is assumed to progress under a constant and uniformly distributed stress in shear:

$$\tau = \text{constant} \quad (8)$$

the value of the constant being equal to the stress at which the stress-strain curve in shear becomes horizontal.

The conditions of perfect symmetry and homogeneity on which equations (6) and (7) are based are not realized in practice. Nor will the conditions underlying (8), i. e., yieldi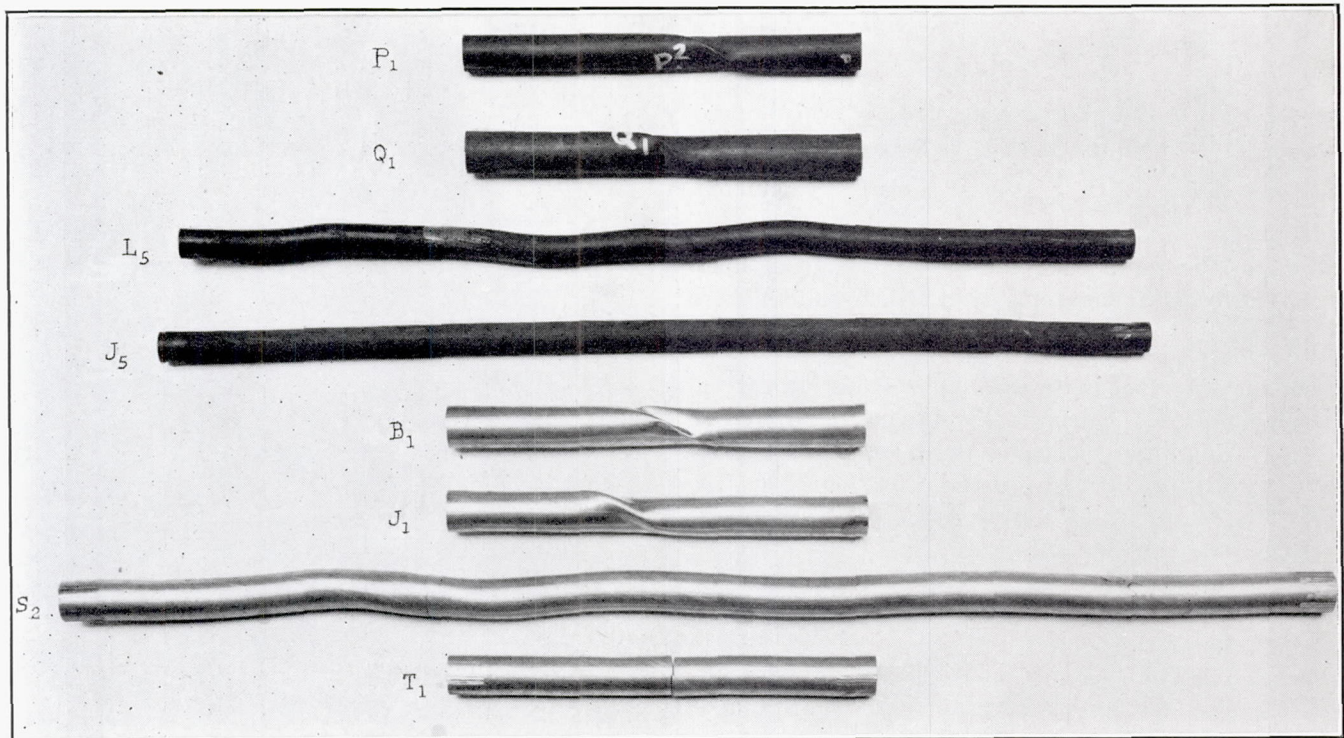ng under constant stress independent of strain, be true for most materials. The equations (6), (7), and (8) represent, therefore, only approximations of practical cases. The degree of approximation for the cases of elastic buckling has been investigated fully in an excellent paper by L. H. Donnell. (See reference 7.) Donnell found that the experimental value of critical shear stress for tubes was roughly 75 percent of the calculated critical stress.

Although equations (6), (7), and (8) are only rough approximations of practical cases, they give a general idea of the effect of different variables upon the torsional strength and upon the type of failure. If they were accurate representations of the behavior of tubes, the stress at failure and the type of failure could be predicted by computations of τ in each of the equations

FIGURE 6.—Appearance of four chromium-molybdenum steel tubes (P₁, Q₁, L₅, J₅) and four 17ST aluminum-alloy tubes (B₁, J₁, S₂, T₁) after completion of torsion test. P₁, B₁ failed by sudden two-lobe buckling; Q₁, J₁ failed by gradual two-lobe buckling; L₅, S₂ failed by helical deformation of the axis; T₁ failed by fracture; J₅ twisted plastically through a large angle and then failed by a slight two-lobe buckle.

(6), (7), and (8). The conditions at failure would be those for which τ is smallest. An analysis of this sort was made for all the tubes tested. Young's modulus E and Poisson's ratio μ were taken equal to the average value given in (12) and (13) on page (11) below. The values of μ, E, t, D, and L being known, the critical shear stresses given by equations (6) and (7) were calculated.

The resulting tabulation of values of τ as given by equations (6) and (7) always showed higher values for helical twisting than for two-lobe buckling. The value of τ for two-lobe buckling lay above the yield strength in shear for 55 out of the 63 steel tubes and for 90 out of the 102 aluminum-alloy tubes. The yield strength in shear was taken as the stress at which the secant modulus of the stress-strain curve in shear was $\frac{5}{6}$ times the initial modulus for the steel tubes and $\frac{6}{7}$ times the initial modulus for the aluminum-alloy tubes. More information concerning the factors $\frac{5}{6}$ and $\frac{6}{7}$ is given later.

For the remaining 8 of the steel tubes and for 3 of the aluminum-alloy tubes the theoretical shear stress for two-lobe buckling lay between that at which the secant modulus of the stress-strain curve in shear deviated by 2 percent from its initial value and the yield strength in shear as just defined. For the remaining 9 of the aluminum-alloy tubes it lay below the stress at which the secant modulus deviated 2 percent from its initial value.

It would not be correct to conclude from this analysis that the shear stress had passed beyond the yield strength in most of the tubes tested before failure took place. That statement would be true only if the critical shear stress for two-lobe buckling could be calculated from (6) up to the yield stress in shear. The critical shear stress is considerably lower than that given by (6) if the stress-strain curve deviates gradually from Hooke's law in approaching the yield strength. However, the analysis did show that considerable yielding must have preceded failure in all but 8 of the steel tubes and all but 12 of the aluminum-alloy tubes. For only 9 of the aluminum-alloy tubes did the analysis predict failure by elastic two-lobe buckling.

It is noteworthy that none of the tubes fell into the category of failure by helical twisting. This result does not exclude this type of failure as a practical possibility. It only indicates that none of the tubes used in the present investigation (maximum length/diameter ratio, $L/D = 80$) were sufficiently long to deform into a helix before failing either by two-lobe buckling or by plastic failure.

Inspection of the tubes after failure (see fig. 6 and tables VII and VIII) indicated that helical twisting did actually occur in some of the thick-wall long tubes and also that in the majority of the tubes the final failure was one of two-lobe buckling. The observed helical failures and also many of the two-lobe failures must have occurred after the yield strength of the material had been reached; i. e., they must be considered as a consequence of the yielding of the material rather than the primary cause of failure.

The conclusion that helical failure, with its dependence on length, must have been secondary is confirmed by a comparison of the shear stress at failure for the 60-inch tubes with that for the 20-inch tubes as given in tables VII and VIII. Only the tubes failing elastically show a consistent tendency toward lower strengths with increase in length. However, this tendency does not indicate the occurrence of helical failure even for the tubes failing elastically. The lowering in strength of the elastic tubes may be explained by the effect of length on the stress producing two-lobe buckling.

If plastic failure and two-lobe failure alone controlled the strength of the tubes, it should be possible to describe the strength of these tubes in terms of the variables determining these types of failure. The maximum median-fiber shear stress in the plastic failure of a thin tube depends primarily on the ultimate strength in shear of the material. In a tube that buckles elastically the maximum median-fiber shear stress will, according to equation (6), vary with the ratio t/D. In the intermediate case of plastic buckling both t/D and the shape of the stress-strain curve in shear beyond the proportional limit are important factors.

No simple relation was found to describe accurately the stress-strain curves of the tubes in shear beyond the proportional limit. An approximate idea of the stress-strain curve may be obtained from a knowledge of both the yield strength in shear τ_{yield} and the ultimate strength in shear τ_{ult}. The ratio of ultimate strength in shear to yield strength in shear may be taken as a measure of the rise in the stress-strain curve beyond the yield point. If this ratio is close to 1.0, the stress-strain curve beyond the yield point will be nearly horizontal while a ratio of 1.4 indicates a considerable rise in stress beyond the yield point; in one case the stress-strain curve will have a sharp knee near the yield point while in the other that knee will be well rounded.

RELATION BETWEEN STRESS-STRAIN CURVES IN SHEAR AND STRESS-STRAIN CURVES IN TENSION

There is still one difficulty in choosing τ_{yield}, τ_{ult} as the two variables that, in addition to the variable t/D, affect the strength of the present group of steel and aluminum-alloy tubes. Neither of these quantities is ordinarily known and both can be determined from torsion tests only when the specimen has sufficiently thick walls so that failure occurs by yielding without any buckling. The properties of the material that are generally known are the yield strength in tension, σ_{yield}, and the ultimate strength in tension, σ_{ult}. It would be possible to substitute these two tensile properties for the two shear properties of the material if a simple relation of sufficient accuracy could be found connecting the two sets of properties.

The existence of such a relation, particularly for the chromium-molybdenum steel tubes, is indicated by the

similarity in shape of stress-strain curves in tension and in shear of specimens cut from the same tube (see figs. 1 and 2.) Theoretical considerations (reference 5, p. 204) indicate that the stress-strain curve in shear may be computed from the stress-strain curve in tension by simply multiplying tensile strains by 1.5 and dividing tensile stresses by $\sqrt{3}$.

The applicability of this relation to the steel tubes was tested by using it to compute for several tubes the stress-strain curves in shear from their tensile stress-strain curves. The measured stress-strain curves in shear and those calculated from the tension tests were found to agree fairly well over their entire range. In most cases it was noticed, however, that the calculated stress-strain curve lay a small distance to the right of the observed curve. A closer degree of coincidence could have been obtained by choosing a value less than 1.5 for the factor by which tensile strains must be multiplied to obtain shear strains. This deviation from the theoretical values is not surprising, since the
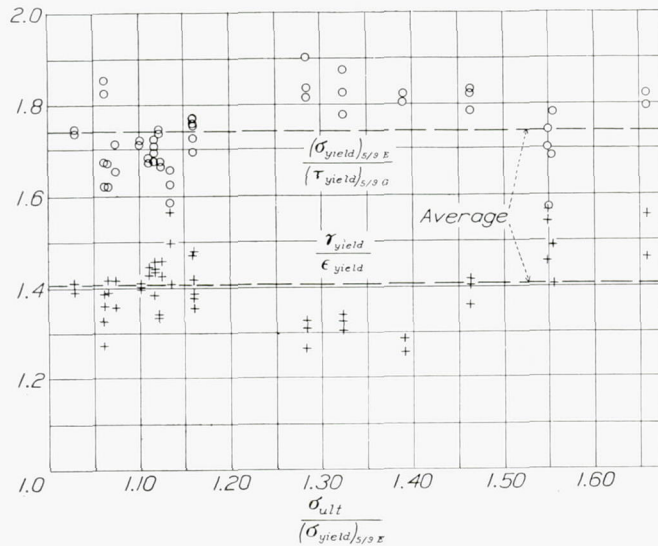

FIGURE 7.—Ratios of yield strengths and yield strains in shear and in tension for chromium-molybdenum steel tubes.

theoretical ratios $\sqrt{3}$ and 1.5 have a sound basis only for an idealized stress-strain curve with an infinitely sharp knee at the yield point and no rise in stress beyond that point. For the same reason one would expect the foregoing ratios not to hold for the aluminum-alloy tubes in which the ratio of ultimate strength to yield strength was not 1, but lay between 1.3 and 1.5.

An estimate of the optimum "factors of affinity" σ/τ and γ/ϵ connecting stress-strain curves in tension and in shear was obtained by plotting the ratios of yield stresses and yield strains $\frac{\sigma_{yield}}{\tau_{yield}}$, $\frac{\gamma_{yield}}{\epsilon_{yield}}$ for each one of the tubes tested using $\frac{\sigma_{ult}}{\sigma_{yield}}$ as abscissa to bring out the variation of the two ratios of affinity with the change in shape of the stress-strain curve beyond the yield strength. (See fig. 7 for steel tubes and fig. 8 for aluminum-alloy tubes.)
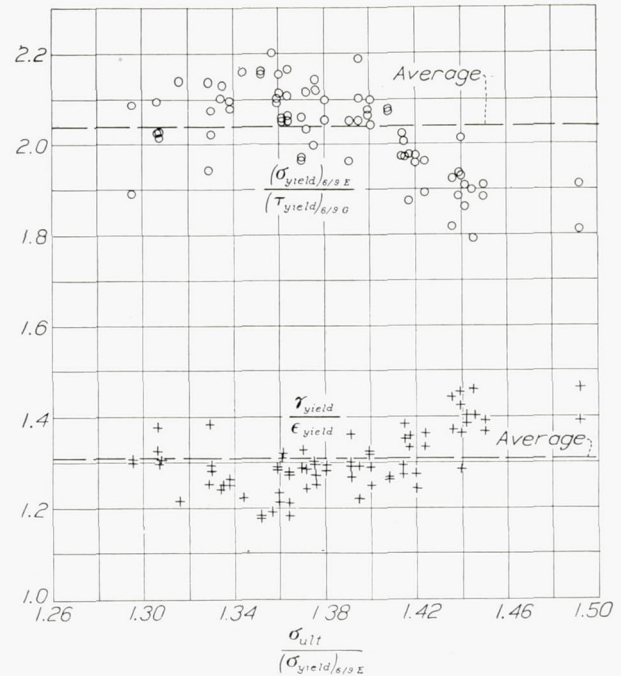

FIGURE 8.—Ratios of yield strengths and yield strains in shear and in tension for 17ST aluminum-alloy tubes.

The yield strength used in these computations was taken as that stress on the stress-strain curve at which the secant modulus was $\frac{5}{9}$ the elastic modulus for the steel tubes and the stress at which it was $\frac{6}{9}$ of the elastic modulus for the aluminum-alloy tubes. The factors $\frac{5}{9}$ and $\frac{6}{9}$ were chosen to give the same value for the tensile yield strength of material just passing Navy Specifications 44T18a and 44T21 (tables I and II) as the yield strength laid down in these specifications (0.2 percent offset), provided the material has a Young's modulus of 30×10^6 pounds per square inch for the steel tubes and one of 10×10^6 pounds per square inch for the aluminum-alloy tubes. The tensile yield strengths computed upon both definitions are listed in tables V and VI. The averages at the bottom of these tables show that the $\frac{5}{9} E$ yield strength is 2 percent higher, on the average, for the chromium-molybdenum steel tubes and that the $\frac{6}{9} E$ yield strength agrees, on the average, within a fraction of 1 percent with the 0.2 percent offset yield strength for the aluminum-alloy tubes. The chief advantage of the $\frac{5}{9} E$ and $\frac{6}{9} E$ yield strengths over the 0.2 percent yield strength is that it will bring the elastic portion of the stress-strain curves in tension into coincidence with the elastic portion of the stress-strain curves in shear if the ordinates and abscissas of the tensile stress-strain curve are multiplied by the factors $\frac{\tau_{yield}}{\sigma_{yield}}$, $\frac{\gamma_{yield}}{\epsilon_{yield}}$, respectively.

For the steel tubes (fig. 7) the ratio $\frac{\sigma_{yield}}{\tau_{yield}}$ scattered within ± 11 percent about an average value of 1.73 while the ratio $\frac{\gamma_{yield}}{\epsilon_{yield}}$ scattered through the same percentage range about an average value of 1.41. There

is a systematic deviation from these average values that becomes a maximum for tubes having $\frac{\sigma_{ult}}{\sigma_{yield}} = 1.3$ approximately. The theoretical affinity ratios $\sqrt{3}$ and 1.5 are fair approximations for the stress-strain curves approaching the idealized shape $\frac{\sigma_{ult}}{\sigma_{yield}} = 1.0$. For the aluminum-alloy tubes (fig. 8) the picture is quite different; the ratio $\frac{\sigma_{ult}}{\sigma_{yield}}$ lies between 1.3 and 1.5. It is not surprising, therefore, that the average affinity ratios are nowhere near the theoretical values $\sqrt{3}$ and 1.5; they are closer to 2 and 1.3. The maximum scatter to each side of these average values is of the order of ±11 percent.
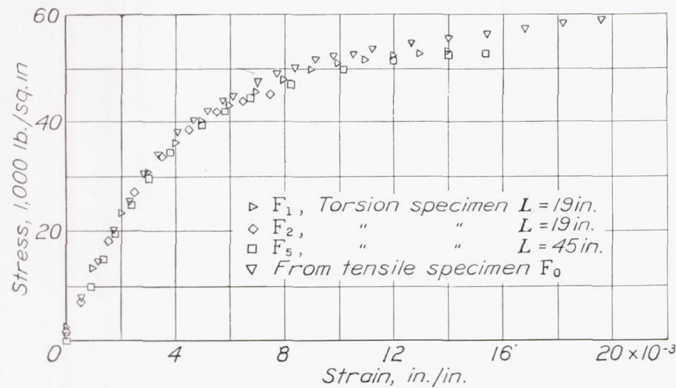

FIGURE 9.—Comparison of stress-strain curves in shear of chromium-molybdenum steel tubes F_0 (1.38 × 0.038 in.) with curve obtained from tensile stress-strain curve by multiplying stresses by $1/\sqrt{3}$ and strains by 1.4.
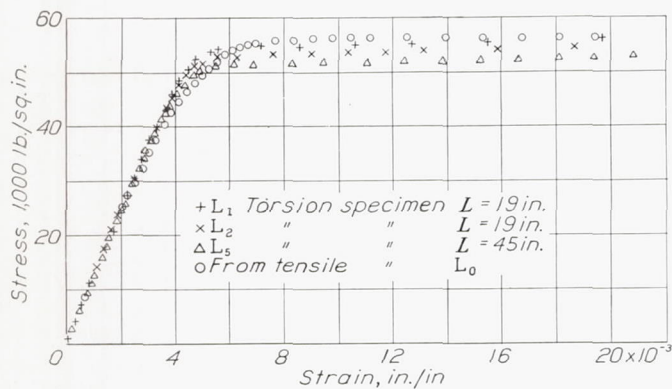

FIGURE 10.—Comparison of stress-strain curves in shear of chromium-molybdenum steel tubes L_0 (1.5 × 0.12 in.) with curve obtained from tensile stress-strain curve by multiplying stresses by $1/\sqrt{3}$ and strains by 1.4.

The usefulness of these approximate affinity relations in predicting the shear stress-strain curve from the tensile stress-strain curve is brought out by figures 9 and 10 for a group of steel tubes and by figures 11 and 12 for a group of aluminum-alloy tubes. These figures show the stress-strain curves in shear as computed from those in tension by multiplying tensile strains by 1.4 for the steel tubes and by 1.3 for the aluminum-alloy tubes and dividing the tensile stresses by $\sqrt{3}$ and 2, respectively. The stress-strain curves in shear as obtained directly from the torque-twist curves are shown for comparison. The calculated curves ap-

proached those obtained from the test data satisfactorily; i. e., within the limits of variations of the different torsion tests, except in the neighborhood of the knee, where the stresses deviated as much as 15 percent for the aluminum-alloy tubes M_1, M_2, M_0 (fig. 11). The greater deviation from affinity for the aluminum-alloy tubes as compared with the steel tubes is also brought out by a comparison of figure 2 with figure 1.
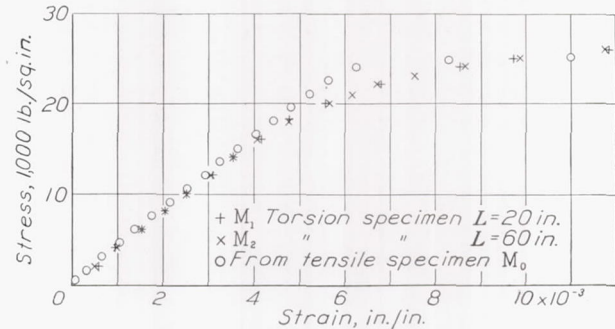
FIGURE 11.—Comparison of stress-strain curves in shear of 17ST aluminum-alloy tubes M_0 (2×0.11 in.) with curve obtained from tensile stress-strain curve by multiplying stresses by 0.5 and strains by 1.3.
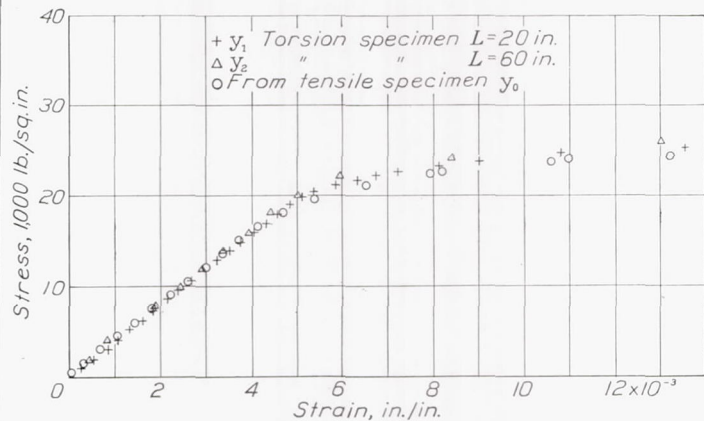
FIGURE 12.—Comparison of stress-strain curves in shear of 17ST aluminum-alloy tubes y_0 (1×0.09 in.) with curve obtained from tensile stress-strain curve by multiplying stresses by 0.5 and strains by 1.3.

VARIATION OF STRENGTH OF TUBES WITH DIMENSIONS AND PHYSICAL PROPERTIES

Variation of stresses at failure.—It has been stated that the tubes tested failed either by plastic torsion, two-lobe buckling, or a failure intermediate between these and that the strength of the tube should therefore depend on the variables determining these three types of failure. For a tube of given metal, i. e., given elastic constants, the length of which is in the range where its effect is negligible, these variables are the wall thickness over diameter ratio t/D, and at least two variables describing the plastic properties in shear of the tube material; e. g., the yield point in shear, τ_{yield} and the ultimate strength in shear, τ_{ult}. In the previous section it was shown that the shear properties and tensile properties of the tube material were roughly affine. The last two variables may therefore be replaced by the corresponding tensile properties, i. e., σ_{yield} and σ_{ult}. In general, then, one would expect that

the maximum shearing stress of the tubes would follow a relation of the type:

$$\tau_{max}=f\left(\frac{t}{D}, \sigma_{yield}, \sigma_{ult}\right) \tag{9}$$

It is necessary to reduce the number of independent variables from 3 to 2 in order to represent the results as a family of curves on a sheet of paper. This reduction may be accomplished by trying various relations between τ_{max} and one of the independent variables and then choosing the one that gives the most consistent behavior for the experimental points. After a number

tubes (fig. 13) show a large scatter throughout the range tested. This result would be expected from the considerable variation in the ratio $\frac{\sigma_{ult}}{\sigma_{yield}}$ and the values of σ_{ult} itself (table V). The points for the aluminum-alloy tubes (fig. 14) fall close to a common curve except for the very thin tubes, which failed by elastic buckling. Figure 14 clearly shows a segregation into the three types of failure that were observed; i. e., failure by elastic two-lobe buckling on the extreme left, failure by a combination of yielding in shear and buckling in the middle, failure in pure shear on the extreme right. The two extreme types of failure are understood fairly

FIGURE 13.—Variation of ratio of shear stress at failure to tensile yield strength with t/D for chromium-molybdenum steel tubes. Straight lines in central region calculated from:

$$15.27\frac{t}{D}\left(\frac{\sigma_{ult}}{\sigma_{yield}}-1\right)+0.981.$$

of trials the most consistent behavior for the steel tubes was found by plotting:

$$\frac{\sqrt{3}\tau_{max}}{\sigma_{yield}}=f\left(\frac{t}{D}, \frac{\sigma_{ult}}{\sigma_{yield}}\right) \tag{10}$$

The factor $\sqrt{3}$ was chosen to make the ordinates close to 1 for most of the tubes.

For the aluminum-alloy tubes it appeared preferable to plot:

$$2\frac{\tau_{max}}{\sigma_{ult}}=f\left(\frac{t}{D}, \frac{\sigma_{ult}}{\sigma_{yield}}\right) \tag{11}$$

The corresponding plots using t/D as abscissa and the term on the left as ordinate are shown in figures 13 and 14 for the two groups of tubes. The points for the steel

well. The theoretical shearing stress at failure for a long tube failing elastically is given by equation (6); for tubes of finite length, it can either be derived from Schwerin's theory (reference 6) or it can be read off directly from the curves computed by Donnell (reference 7). (The three curves shown for elastic two-lobe buckling in figs. 13 and 14 correspond to minimum, average, and maximum values of σ_{yield} and σ_{ult}, respectively, as measured for the tubes tested.)

Figures 13 and 14 show that no more than 7 of the steel tubes and no more than 20 of the aluminum-alloy tubes can be considered as having failed by elastic buckling; this number includes the tubes lying in the transition region between elastic failure and combined failure as well as those definitely to the left of it. The
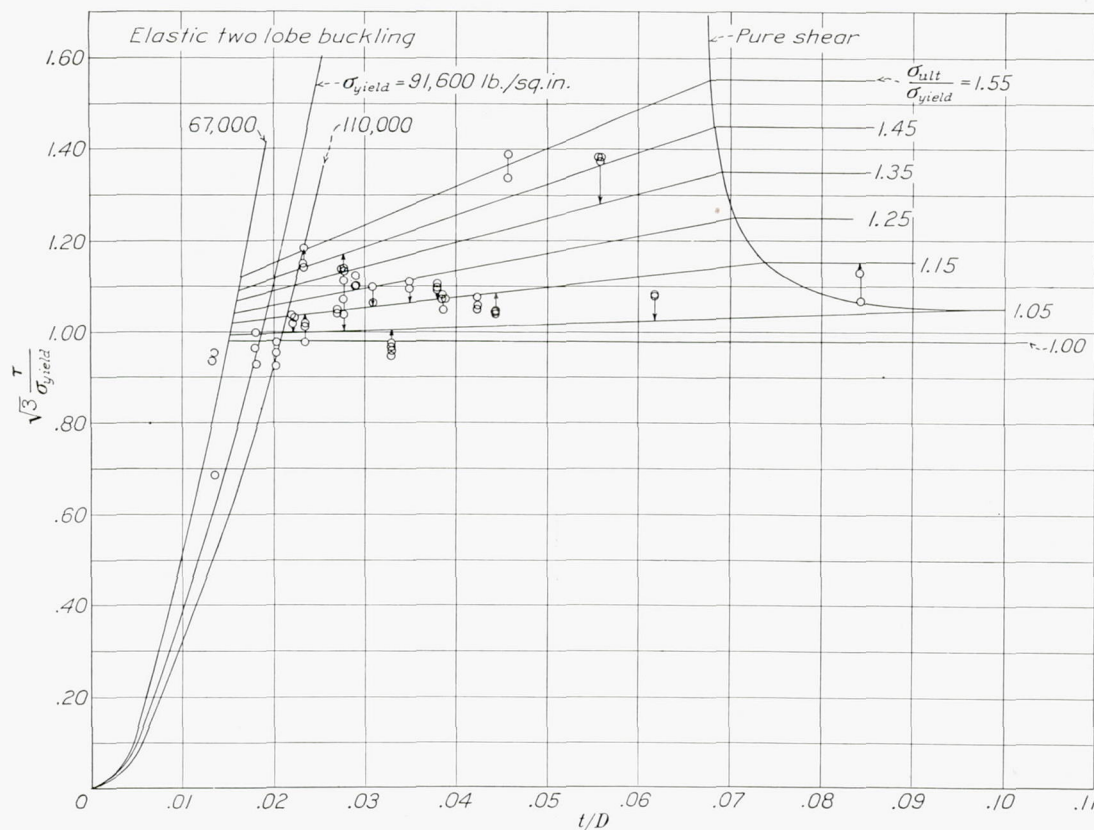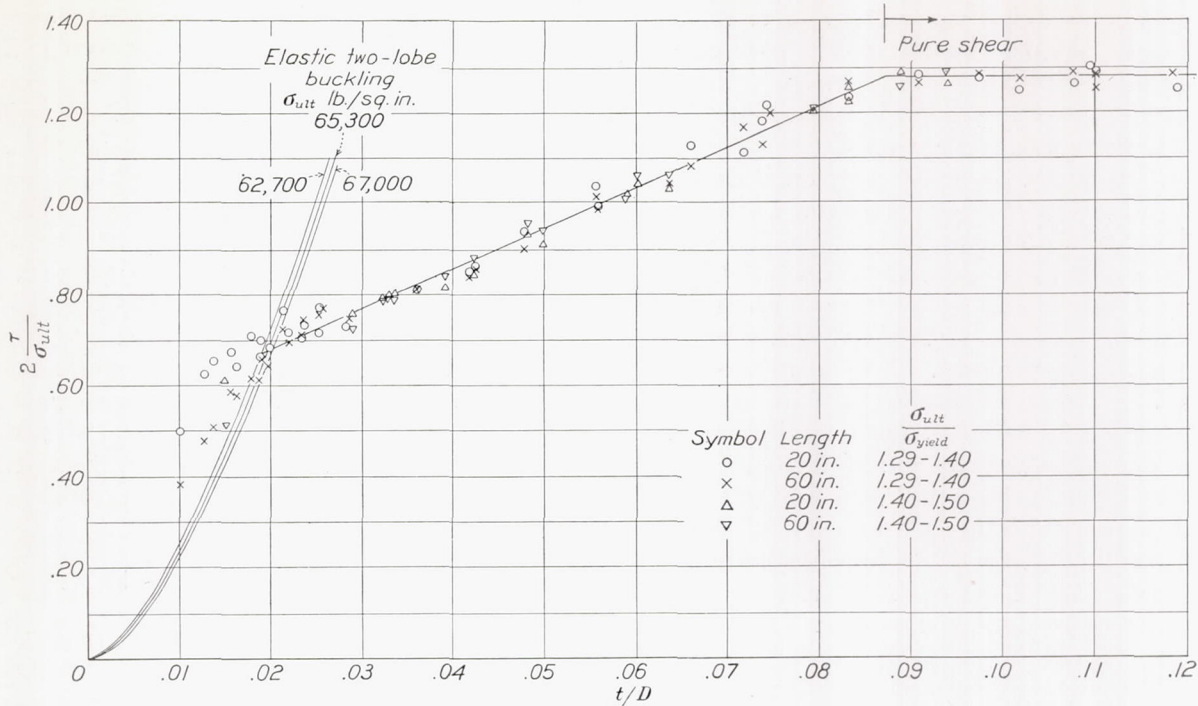
FIGURE 14.—Variation of ratio of shear stress at failure to tensile strength with t/D for 17ST aluminum-alloy tubes. Straight line in central region calculated from:

$$2\frac{\tau}{\sigma_{ult}}=8.96\frac{t}{D}+0.501.$$

approximate analysis in an earlier section of this paper had predicted that 8 of the steel tubes and 11 of the aluminum-alloy tubes should have fallen into this category. The agreement, though not close, is sufficient considering the uncertainty of the assumptions made, especially those relative to the limit above which combined failure must be expected.

In every case of elastic buckling the long tubes failed at a lower stress than the short ones, the difference exceeding 30 percent in some cases. Schwerin's formula for long tubes (equation (6)) is not sufficient, therefore, to describe the strength of the short tubes failing elastically. An adequate comparison with the theory must include the effect of length as considered in general by Schwerin (reference 6) and in detail by Donnell (reference 7). Donnell has shown that the effect of length L, thickness t, and diameter D on the strength in torsion of an elastic tube may be represented on a single curve by plotting

$$B=\sqrt{1-\mu^2}\,\frac{\tau}{E}\,\frac{L}{t}$$

as a function of

$$J=\frac{1}{\sqrt{1-\mu^2}}\frac{L^2t}{D^3}$$

Figure 15 shows the curves derived by Donnell for tubes with hinged edges and with clamped edges together with Schwerin's curve for infinitely long tubes. The individual points represent the observed values of $B=f(J)$ computed from the observed shear stress at failure and the dimensions of the tube and the following elastic constants: for chromium-molybdenum steel tubes,

$E=28,600,000$ pounds per square inch, $\mu=0.235$, (12)

for 17ST aluminum-alloy tubes,

$E=10,430,000$ pounds per square inch, $\mu=0.319$. (13)
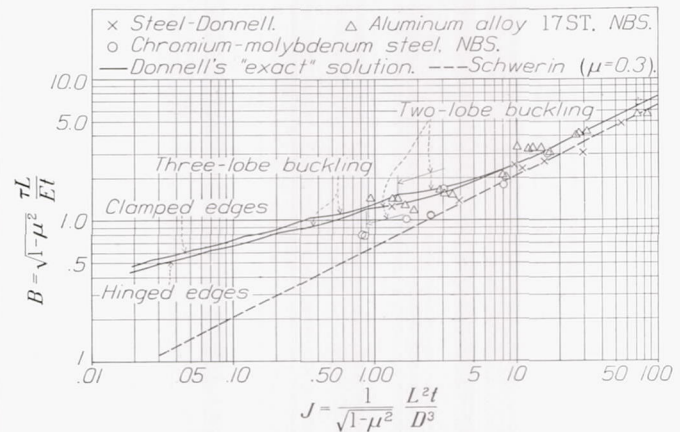
FIGURE 15.—Comparison of observed shear stress at failure of tubes that failed by elastic buckling with theoretical values given by Donnell and Schwerin.

The Young's moduli represent average values of the modulus measured in the tension test (tables V and VI). The values for Poisson's ratio represent an average of values calculated for each size of tube from the well-known relation $\mu=\frac{E}{2G}-1$. This relation is strictly true only for perfectly isotropic material obeying Hooke's Law. The relatively low value of μ for the steel tubes may be due partly to lack of isotropy of the material. It did not seem worth while to investigate this in view of the small effect of a change in μ on the critical stress of a thin tube as given by figure 15. The

points for the steel tubes are scattered over the same region as those obtained by Donnell in tests on steel tubes buckling with two lobes (crosses); they are on the average about 25 percent below the curve for a tube with hinged edges. The points for the aluminum-alloy tubes are somewhat higher, scattering through a range of about ±25 percent about the curve with hinged edges. A few points fell into the border region between two-lobe and three-lobe failure. Examination of the corresponding tubes indicated a failure which may have started with three lobes but which ended with two lobes as the deformation increased. No definite reason can be assigned for the greater strengths of the aluminum-alloy tubes; possibly the closer tolerances within which the tubes are manufactured permit them to develop more nearly the full theoretical strength of the ideal tube. All of the tubes except one showed strengths greater than that given by Schwerin's formula for infinitely long tubes. Donnell's curve for hinged edges may, therefore, be taken as a fair estimate of the probable strength of the tubes failing elastically while Schwerin's formula may be used to give a lower limit of their strength.

Failure in plastic shear may be expected when the shear stress reaches a value equal to the ultimate shear strength, τ_{ult}, of the material. In the case of the steel tubes (fig. 13) this assumption leads to a family of horizontal straight lines having the ordinate

$$\frac{\sqrt{3}\,\tau}{\sigma_{yield}} = \frac{\sqrt{3}\,\tau_{ult}}{\sigma_{ult}}\frac{\sigma_{ult}}{\sigma_{yield}}.$$

Only 2 of the 63 steel tubes tested fell into the region of failure in pure shear. These two were insufficient to establish a value for the ratio τ_{ult}/σ_{ult}. In the absence of adequate test data it was decided to assume this ratio to be the same as that of the yield strengths:

$$\tau_{ult} = \frac{1}{\sqrt{3}}\,\sigma_{ult} = 0.577\,\sigma_{ult}. \qquad (14)$$

This assumption is believed to be conservative since the corresponding ratio of ultimate stresses for the aluminum-alloy tubes was found to be about 10 percent higher; i. e., 0.64. Converting equation (14) into the ordinates used in figure 13 gives the family of horizontal lines:

$$\sqrt{3}\,\frac{\tau_{ult}}{\sigma_{yield}} = \frac{\sigma_{ult}}{\sigma_{yield}}.$$

In the case of the aluminum-alloy tubes (fig. 14) 18 of the points fall into the region of plastic shear. They scatter about a common horizontal line with the ordinate

$$2\,\frac{\tau}{\sigma_{ult}} = 1.28. \qquad (15)$$

For the aluminum-alloy tubes, therefore, the ultimate strength in plastic shear is about 64 percent of the ultimate strength in tension.

It is seen, after drawing the curves corresponding to elastic failure for a long tube as given by equation (6) and the horizontal straight lines corresponding to failure by plastic shear, that most of the points fall into the intermediate region. For the aluminum-alloy tubes the individual points seem to fall about a common straight line increasing with the t/D ratio. The points for the steel tubes in figure 13 show too great a scatter to suggest the type of variation with t/D at a glance; however, it appears, after segregating the points into groups with nearly constant ratio $\sigma_{ult}/\sigma_{yield}$ that a linear increase with t/D is the simplest variation that gives an approximate fit. It remains to find an empirical relation between the stress ratio at failure and the ratio $\sigma_{ult}/\sigma_{yield}$. A number of formulas were tried and the best fit was obtained with a formula of the type:

$$\frac{\sqrt{3}\,\tau}{\sigma_{yield}} = a\,\frac{t}{D}\left(\frac{\sigma_{ult}}{\sigma_{yield}} - 1\right) + b \qquad (16)$$

where a and b are constants. Evaluating these constants by least squares gave $a = 15.27$ and $b = 0.981$ so that the stress ratio at failure of the chromium-molybdenum steel tubes buckling plastically may be expressed by the empirical formula:

$$\frac{\sqrt{3}\,\tau}{\sigma_{yield}} = 15.27\,\frac{t}{D}\left(\frac{\sigma_{ult}}{\sigma_{yield}} - 1\right) + 0.981, \begin{array}{c}\left(0.02 < \dfrac{t}{D} < 0.07\right)\\ (L/D \leq 80).\end{array} \qquad (17)$$

The stress ratios calculated from this formula are plotted against the observed stress ratios in figure 16. The points scatter about 5 percent to either side of the
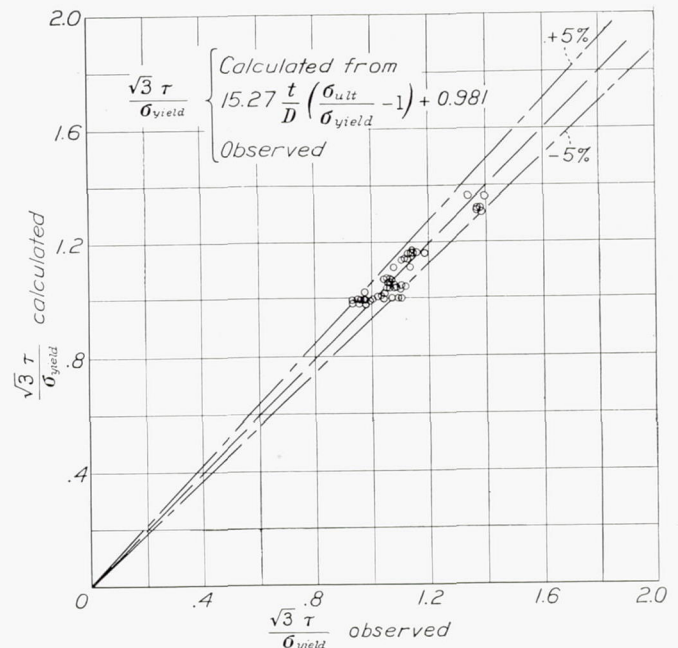
FIGURE 16.—Comparison of calculated and observed stress ratios for chromium-molybdenum steel tubes.

line of exact agreement. The corresponding empirical formula for the plastic buckling of the aluminum-alloy tubes was also evaluated with the help of least squares; it may be written as:

$$\frac{\tau}{\sigma_{ult}}=4.48\frac{t}{D}+0.2506, \left(0.022<\frac{t}{D}<0.085, \frac{L}{D}\leq 60\right). \quad (18)$$

The lower limit of $\frac{t}{D}=0.022$ corresponds to the cut-off

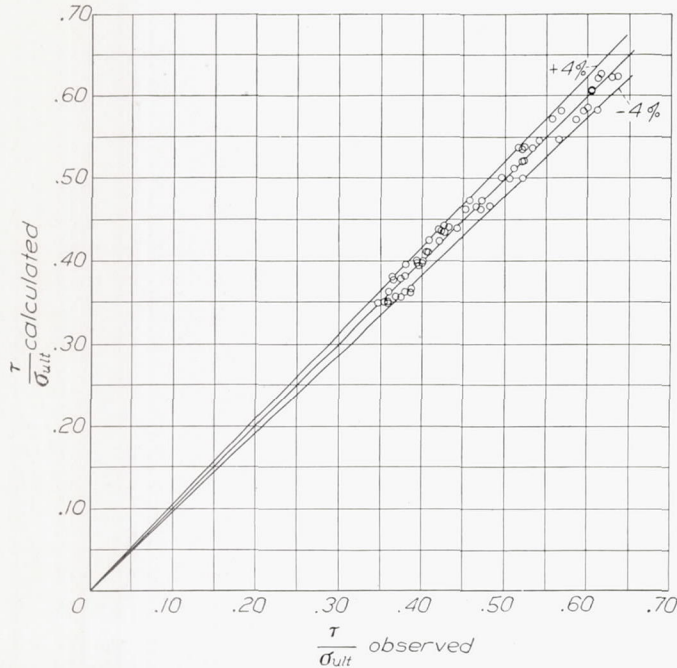of the empirical formula by Schwerin's curve for long tubes. Data on torsion tests of short tubes kindly

FIGURE 17.—Comparison of calculated and observed stress ratios for 17ST aluminum-alloy tubes:

$$\frac{\tau}{\sigma_{ult}}=4.48\frac{t}{D}+0.2506$$

for, $0.022<\frac{t}{D}<0.085$.

supplied by the Aluminum Company of America indicate that the cut-off for short tubes can be moved

to smaller values of $\frac{t}{D}$. The tests made by the Aluminum

Company of America (Physical Test Report No. 31–40)

on 13 17ST tubes having a $\frac{t}{D}$ ratio ranging from 0.0095

to 0.02 and an $\frac{L}{D}=4.8$, indicate that the straight line

(18) may be extended to the left down to $\frac{t}{D}=0.09$ at

which point it is cut off by Donnell's curve (see fig. 15)

for $\frac{L}{D}=4.8$. Tests on 23 further tubes with $\frac{L}{D}=7$ and

with $\frac{t}{D}$ ranging from 0.018 to 0.099 were found to scatter

uniformly about the straight lines given by (18) and (15). The stress ratios calculated from formula (18) are compared with the observed stress ratios in figure 17.

The individual points scatter about 4 percent to either side of the line of exact agreement.

Design charts for twisting moment producing failure.—Designers are usually more interested in expressing the torsional strength of a tube in terms of torque at failure rather than in terms of the mean fiber stress τ at failure. The value of τ had originally been derived from M by relation (5), so that τ and M are connected by the formula:

$$M=\frac{\pi D^3}{2}\frac{t}{D}\left(1-\frac{2t}{D}+2\left(\frac{t}{D}\right)^2\right)\tau. \quad (19)$$

Formulas for M for the three types of failure may be obtained from equation (19) by substituting for τ the value obtained from Donnell's work (fig. 15) for the case of elastic failure, from equations (17) and (18) for the case of combined failure, and from equations (14) and (15) for the case of plastic failure.

Elastic failure by two-lobe buckling depends, according to Donnell, on the length as well as on the wall-thickness ratio t/D of the tube. For long tubes (fig. 15) the length effect is small, however, and the actual strength of the tube will be only a few percent greater than that given by Schwerin's formula (6) in which the length does not enter.

Substituting equations (6), (17), (14), and (12) in equation (19) gives the following formulas for the twisting torque at failure of the chromium-molybdenum steel tubes: two-lobe buckling failure of a long tube:

$$\frac{M}{D^3\sigma_{yield}}=\frac{3.11\times 10^7}{\sigma_{yield}}\left(\frac{t}{D}\right)^{5/2}\left(1+0.4\frac{t}{D}\right), \quad (20)$$

$$\left(0\leq\frac{t}{D}\leq 0.024\right),$$

combined plastic failure and buckling:

$$\frac{M}{D^3\sigma_{yield}}=0.908\left(\frac{t}{D}\right)\left(1-2\frac{t}{D}+2\frac{t^2}{D^2}\right)\left[15.27\frac{t}{D}\left(\frac{\sigma_{ult}}{\sigma_{yield}}-1\right)\right.$$
$$\left.+0.981\right], \left(0.015>\frac{t}{D}>0.092\right), \quad (21)$$

failure in pure shear:

$$\frac{M}{D^3\sigma_{yield}}=0.908\frac{t}{D}\left(1-2\frac{t}{D}+2\frac{t^2}{D^2}\right)\frac{\sigma_{ult}}{\sigma_{yield}}, \quad (22)$$

$$\left(0.068<\frac{t}{D}<0.100\right).$$

The ranges of t/D for which each one of these formulas holds overlap because the boundary between the different types of failure depends on σ_{yield} and σ_{ult} in addition to t/D. The proper type of formula to use in any given case is the one that gives the lowest twisting moment M. In the special case of a material for which $\sigma_{ult}=\sigma_{yield}$, it is seen that combined failure according to equation (21) should always occur in preference to failure in pure shear, the torque for combined failure being about 2 percent less than that for pure shear. Actually the 2 percent variation is not significant; the experimental scatter of points would produce an uncertainty of this

order in the fitting of the empirical relation (17) by least squares. For material having a stress-strain curve such that $\sigma_{ult}=\sigma_{yield}$ equations (21) and (22) should coincide since a tube of such material would not be able to carry more than the yield stress in torsion of the material.

The equations (20), (21), and (22) cannot be expressed in Cartesian coordinates as a single curve or even as a family of curves because they contain the four variables $\dfrac{M}{D^3\sigma_{yield}}$, $\dfrac{t}{D}$, $\dfrac{\sigma_{ult}}{\sigma_{yield}}$, and σ_{yield}. In order to show them as a single curve in a nomographic chart connecting the first three variables, σ_{yield} must be expressed as a function of $\dfrac{\sigma_{ult}}{\sigma_{yield}}$ of a type form;

$$\sigma_{yield}=\frac{1}{c_0\left(\dfrac{\sigma_{ult}}{\sigma_{yield}}-1\right)+c_1} \tag{23}$$

which converts equation (20) into the same type form as equation (21). Evaluating c_0 and c_1 to give the best fit to the observed values of the tensile yield strengths plotted as a function of $\dfrac{\sigma_{ult}}{\sigma_{yield}}$ gave the following relation for (23):

$$\sigma_{yield}=\frac{10^6}{6.62\left(\dfrac{\sigma_{ult}}{\sigma_{yield}}-1\right)+9.79}. \tag{24}$$

Figure 18 shows the nomogram that was derived from equations (21) and (22) after substituting equation (24) in (20). Two examples illustrate the use of this nomogram.

1. Find the wall thickness of a 2-inch chromium-molybdenum steel tube 4 feet long that will fail when subjected to a torque of 2,500 lb.-ft. The tensile yield strength of the tube material is 80,000 pounds per square inch and its tensile ultimate strength is 100,000 pounds per square inch.

Answer. The tube falls within the range of dimensions and properties of those tested so that figure 18 may be applied to compute its wall thickness.

$$\frac{\sigma_{ult}}{\sigma_{yield}}=\frac{100000}{80000}=1.25$$

$$\frac{M}{D^3\sigma_{yield}}=\frac{2500\times12}{2^3(80000)}=0.0469$$

Connecting these points on the nomogram (dotted line, fig. 18) gives:

$$\frac{t}{D}=0.0487,\ t=2\times0.0487=0.0974\text{ inch.}$$

Failure by combined plastic shear and buckling may be expected.

2. Find the wall thickness of a 1½ inch chromium-molybdenum steel tube 5 feet long that will fail when subjected to a torque of 600 lb.-ft. The tensile yield strength of the tube material is 75,000 pounds per square inch and its tensile ultimate strength is 95,000 pounds per square inch.

Answer. The tube falls within the range of dimensions and properties of those tested so that figure 18 may be applied to compute it.

$$\frac{\sigma_{ult}}{\sigma_{yield}}=\frac{95,000}{75,000}=1.267$$

$$\frac{M}{D^3\sigma_{yield}}=\frac{600\times12}{1.5^3\times75,000}=0.0284$$

Connecting these points on the nomogram (dotted line, fig. 18) gives two intersections as follows:

$$\frac{t}{D}=0.0229,\ \frac{t}{D}=0.0302.$$

The first value corresponds to two-lobe buckling as a long tube and the second, to combined failure. A heavier tube is required to resist combined failure than to resist buckling; hence combined failure is more likely to occur. The wall thickness must be chosen as

$$t=1.5\times0.0302=0.0453\text{ inch.}$$

Frequently material is required to satisfy certain specifications for minimum yield strength and tensile strength.

Design curves for such material may easily be derived either from equations (20), (21), and (22) or from figure 18 by the substitution of the specified values of σ_{ult} and σ_{yield}. Figure 19 shows a design chart for determining the size of chromium-molybdenum steel tubes 19 to 60 inches in length that just meet the minimum requirements of Navy Specifications 44T18 and 44T18a (table I).

The material of the tube specified in problem 2 just meets Navy Specification 44T18a. The curve of figure 19 can, therefore, be applied directly to solve problem 2.

$$\frac{M}{D^3}=\frac{600\times12}{1.5^3}=\frac{7,200}{3.375}=2,130\text{ lb./sq. in.}$$

The ordinate $\dfrac{T}{D^3}=2,130$ intersects curve B at $\dfrac{t}{D}=0.03$.

A vertical through the point of intersection extending into the lower half of the chart intersects the inclined line for $D=1.5$ inch at a value of $t=0.045$ inch. This solution coincides with the one obtained from the nomogram of figure 18.

Design charts for the aluminum-alloy tubes may be obtained by substituting the expressions for critical stress given by equations (6), (18), and (15) into equation (19). If, in addition, the values given in equation (13) for the elastic constants E and μ are substituted, the following three equations are obtained for the torque at failure.

For elastic two-lobe buckling of a long tube according to Schwerin:

$$\frac{M}{D^3\sigma_{ult}}=\frac{1.2\times10^7}{\sigma_{ult}}\left(\frac{t}{D}\right)^{5/2}\left(1+0.4\frac{t}{D}\right),\ \left(0<\frac{t}{D}<0.02\right), \tag{25}$$
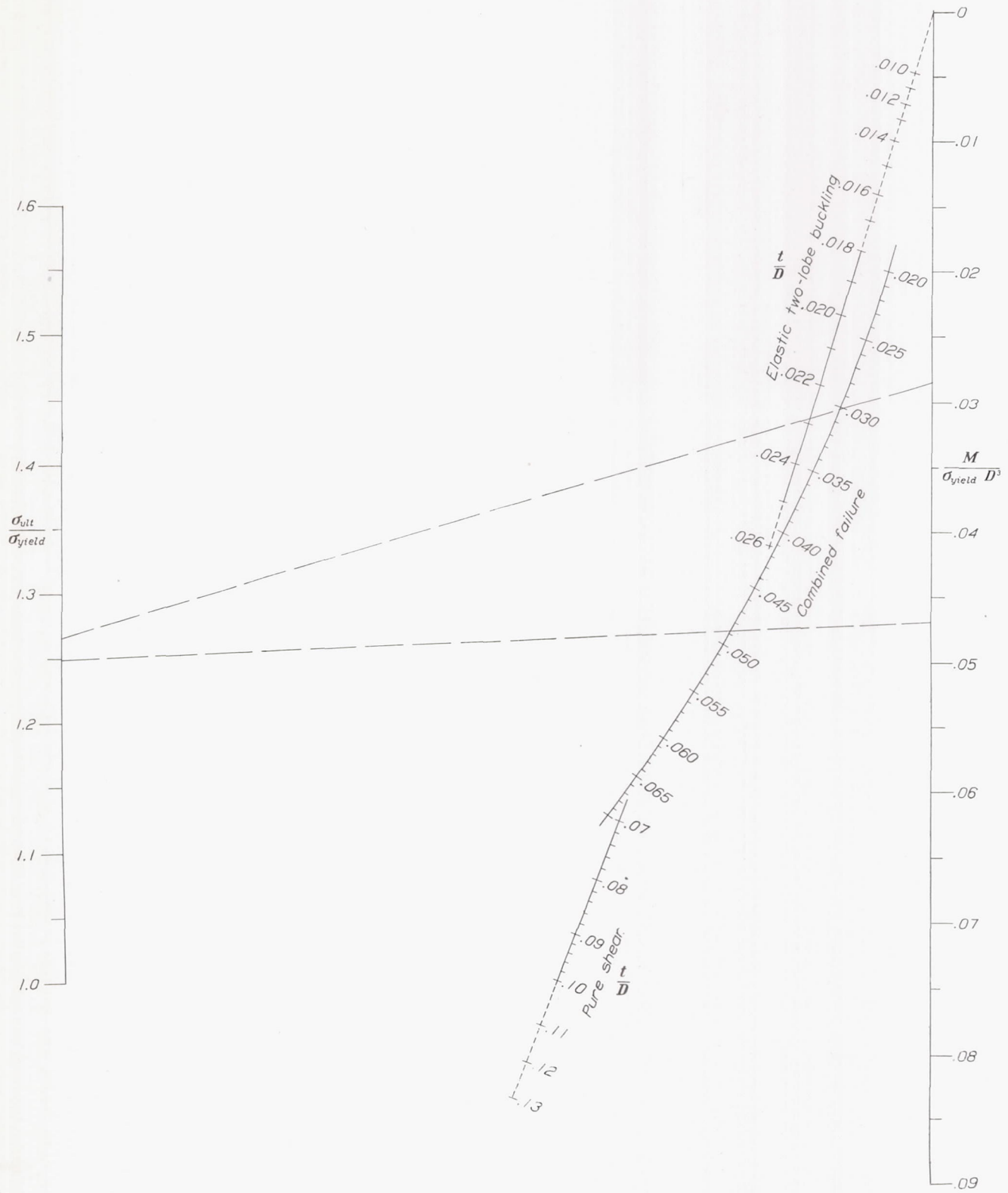
FIGURE 18.—Nomographic design chart for torsional strength of chromium-molybdenum steel tubes 19–60 inches long.
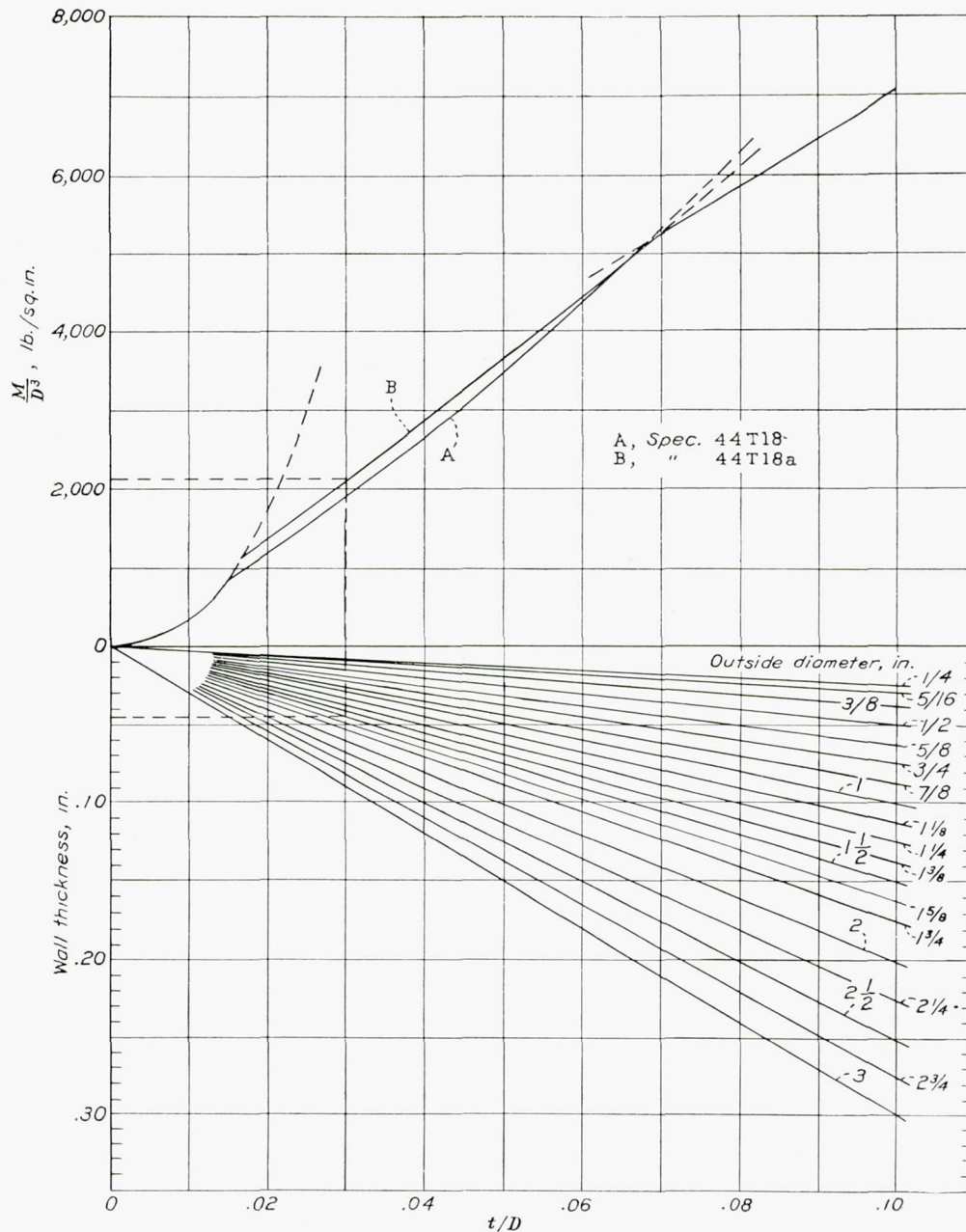
FIGURE 19.—Design chart for torsional strength of chromium-molybdenum steel tubes 19–60 inches long satisfying Navy Specification 44T18 (σ_{ult}=95,000 lb./sq. in., σ_{yield}=60,000 lb./sq. in.) and Navy Specification 44T18a (σ_{ult}=95,000 lb./sq. in., σ_{yield}=75,000 lb./sq. in.).

for combined plastic failure and two-lobe buckling:

$$\frac{M}{D^3\sigma_{ult}}=0.394\left(\frac{t}{D}\right)\left(1+15.9\frac{t}{D}-33.7\frac{t^2}{D^2}\right),$$

$$\left(0.02<\frac{t}{D}<0.088\right), \tag{26}$$

for failure in pure shear:

$$\frac{M}{D^3\sigma_{ult}}=1.005\left(\frac{t}{D}\right)\left(1-2\frac{t}{D}+2\frac{t^2}{D^2}\right),$$

$$\left(0.088<\frac{t}{D}<0.12\right). \tag{27}$$

The strength of the aluminum-alloy tubes can, accord-

ingly, be described with the help of the three variables $\frac{M}{D^3\sigma_{ult}}$, σ_{ult}, and $\frac{t}{D}$. Only the two variables $\frac{M}{D^3\sigma_{ult}}$ and $\frac{t}{D}$ are needed if curves of (25) are plotted for given values of σ_{ult} as in figure 14. This procedure results in figure 20. A simple example will illustrate the use of these curves.

Find the wall thickness of a 2-inch 17ST aluminum-alloy tube 5 feet long that will fail when subjected to a torque of 2,000 lb.-ft. The tensile strength of the tube material is 68,000 pounds per square inch.

Answer.—The tube falls within the range of dimensions and properties of those tested so that figure 20 may be applied to compute it.
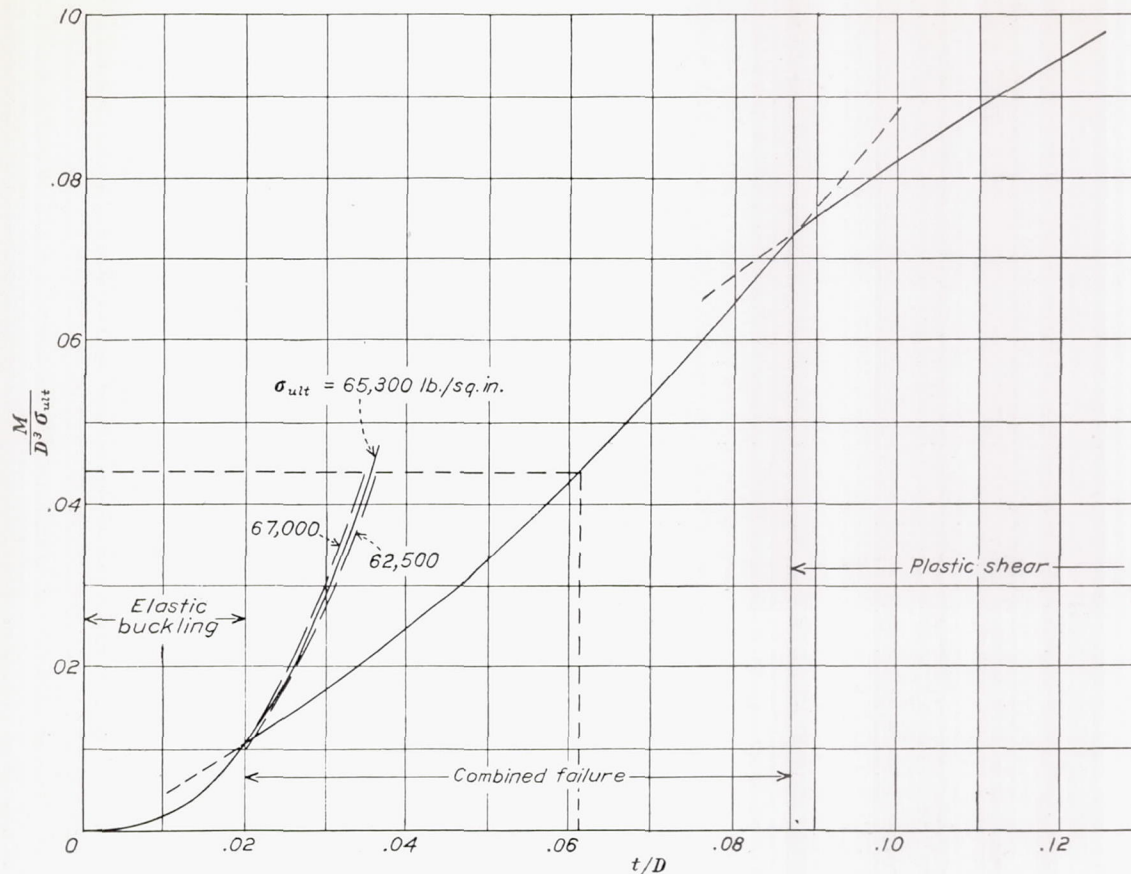
FIGURE 20.—Design chart for torsional strength of 17ST aluminum-alloy tubes.

$$\frac{M}{D^3 \sigma_{ult}} = \frac{2,000 \times 12}{2^3 \times 68,000} = 0.0441$$

According to figure 20, this corresponds to

$$\frac{t}{D} = 0.061, \; t = 0.061 \times 2 = 0.122 \text{ inch.}$$

The wall thickness of the tube that may be expected to fail under about 2,000 lb.-ft. torque would be 0.122 inch.

A design chart similar to figure 19 may be derived from figure 20 for aluminum-alloy material required to satisfy certain specifications for minimum tensile strength. Figure 21 shows such a chart for 17ST tubing complying with Navy Specification 44T21 (table II); the upper half of the figure was constructed from figure 20 by substituting 55,000 pounds per square inch for σ_{ult}, while the lower half is a set of straight lines corresponding to commercially available diameters of 17ST tubing. The following example illustrates the use of figure 21.

Find the wall thickness of a 2-inch 17ST aluminum-alloy tube 5 feet long that will fail when subjected to a torque of 1,000 lb.-ft. The material of the tube shall just meet Navy Specification 44T21.

The tube falls within the range of dimensions and properties of those tested so that figure 21 may be applied to compute it.

$$\frac{M}{D^3} = \frac{1000 \times 12}{2^3} = 1,500$$

It is seen that by following the dotted line in figure 21 that this value corresponds to a wall thickness of $t = 0.086$ inch in a tube 2 inches in diameter.

REFERENCES

1. Otey, N. S.: Torsional Strength of Nickel Steel and Duralumin Tubing as Affected by the Ratio of Diameter to Gage Thickness. T. N. No. 189, N. A. C. A., 1924.
2. The Allowable Stress in Tubes Subjected to Torsion. A. C. I. C. No. 641, Matériel Division, Army Air Corps, 1929.
3. Templin, R. L., and Moore, R. L.: Specimens for Torsion Tests of Metals. A. S. T. M. Proc., Part II, 30, 1930, pp. 534–543.
4. Fuller, Forrest B.: The Torsional Strength of Solid and Hollow Cylindrical Sections of Heat-Treated Alloy Steel. Jour. Aero. Sci., vol. III, no. 7, May 1936, pp. 248–251.
5. Nadai, A.: Plasticity. McGraw-Hill Book Co., Inc., 1931.
6. Schwerin, E.: Die Torsionsstabilität des dünnwandigen Rohres. Z. f. a. M. M., vol. V, no. 3, June 1925, pp. 235–243.
7. Donnell, L. H.: Stability of Thin-Walled Tubes Under Torsion. T. R. No. 479, N. A. C. A., 1933.

FIGURE 21.—Design chart for torsional strength of 17ST aluminum-alloy tubes 19–60 inches long satisfying Navy Specification 44T21a ($\sigma_{ult}=55,000$ lb./sq. in.).

TABLE V.—TENSILE AND HARDNESS PROPERTIES OF CHROMIUM-MOLYBDENUM STEEL TUBES

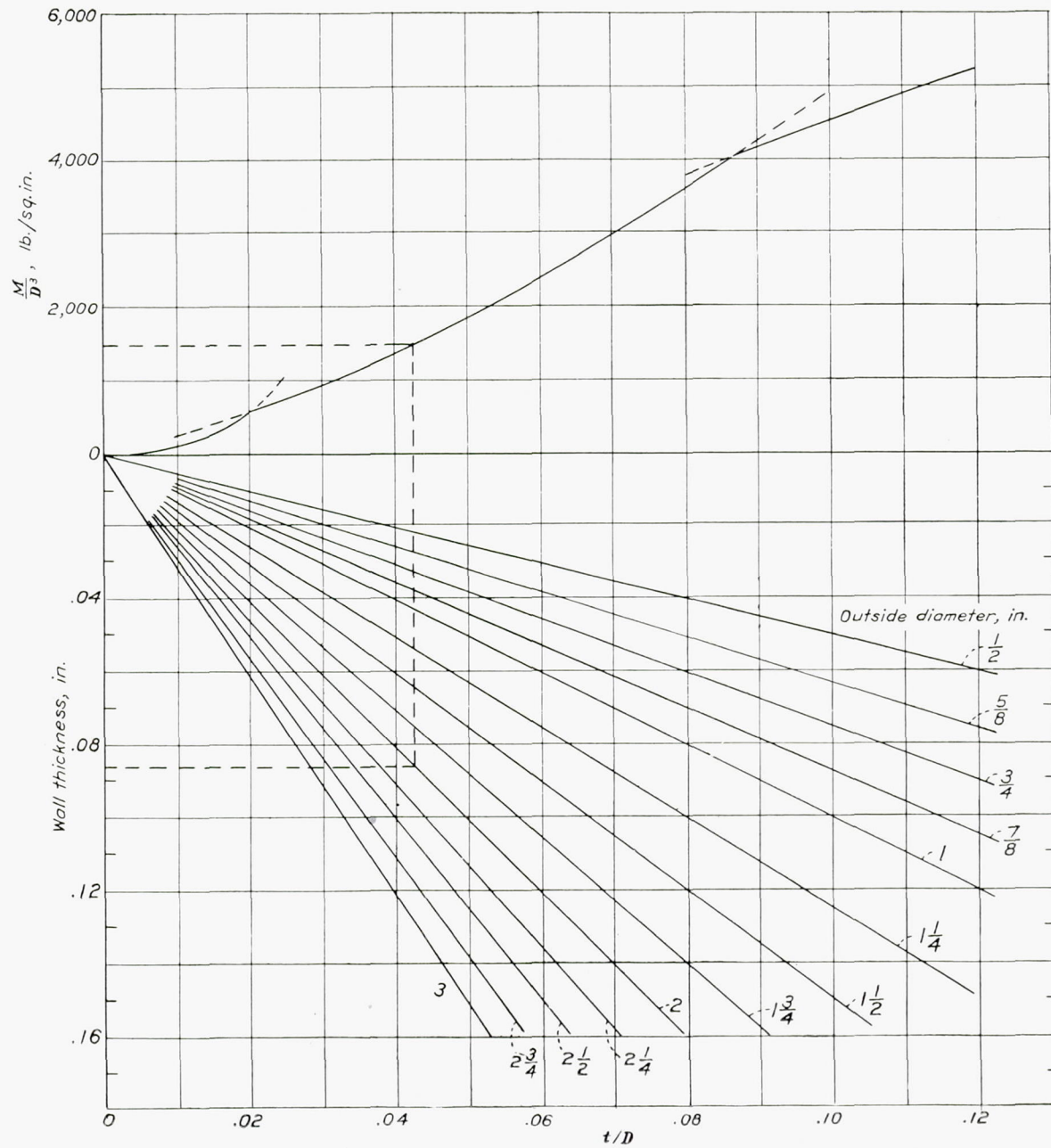| Speci-men	Nominal size (in.)	Yield strength		Tensile strength (lb./sq. in.)	Elonga-tion in 2 inches (percent)	Vickers numbers [b]		Young's modulus (lb./sq. in.)	Tensile strength / Yield strength
		0.002 [a] (lb./sq. in.)	5/9 E (lb./sq. in.)			Left end	Right end		
A₀	¾×0.028	84,000	84,300	97,400	23.0	209	224	29.9×10⁶	[c] 1.16
B₀	1 × .035	89,000	91,000	101,000	18.0	216	214	28.8	1.14
C₀	1⅛× .049	93,000	93,500	102,500	12.5	224	213	29.0	1.10
D₀	1½× .058	99,000	100,000	110,700	18.5	249	240	29.1	1.12
E₀	2 × .065	108,000	109,500	114,800	18.5	264	253	28.7	1.06
F₀	1⅜× .035	81,000	84,000	118,700	17.2	263	264	28.8	1.46
G₀	1½× .035	69,200	69,000	107,300	28.5	260	260	29.0	1.55
H₀	1½× .049	78,600	79,400	88,400	17.0	214	204	28.5	1.12
I₀	1½× .065	67,700	67,700	105,300	32.0	206	214	28.6	1.56
J₀	1½× .083	82,200	85,500	114,300	24.0	262	263	28.8	1.39
K₀	1½× .095	110,000	110,500	113,300	16.8	243	242	28.8	1.03
L₀	1½× .120	96,000	97,000	106,700	26.0	236	232	28.5	1.11
M₀	1⅝× .049	90,500	91,100	96,600	16.0	241	266	27.3	1.07
N₀	1¾× .049	96,800	103,600	132,900	19.0	296	311	27.6	1.37
O₀	1⅝× .035	93,000	93,300	100,300	14.0	240	274	27.5	1.08
P₀	1¾× .035	105,000	105,300	109,700	16.0	283	262	27.6	1.04
Q₀	2 × .035	99,100	101,000	109,200	11.5	264	245	27.6	1.10
R₀	1⅛× .035	95,200	95,900	101,700	14.0	254	248	29.0	1.07
S₀	1¼× .035	87,800	88,200	98,200	16.0	252	239	28.4	1.12
T₀	1½× .035	93,800	95,500	107,400	17.0	245	232	28.2	1.14
U₀	1½× .049	103,800	105,300	122,000	15.0	272	270	28.8	1.18
V₀	2½× .032	75,000	73,000	122,500	24.0	281	270	30.2	1.63
Average (22 speci-mens)		90,800	92,900	108,200	18.8	249	247	28.6	1.208

[a] Stress at which strain exceeds $\frac{stress}{30\times10^6}$ by 0.002, in./in.
[b] Vickers numbers for 10-kg weight.
[c] Based on 0.002 yield strength.

TABLE VI.—TENSILE AND HARDNESS PROPERTIES OF 17ST ALUMINUM-ALLOY TUBES

Speci-men	Nominal size (in.)	Yield strength		Tensile strength (lb./sq. in.)	Elonga-tion in 2 inches (per-cent)	Vickers numbers [b]		Young's modulus (lb./sq. in.)	Tensile strength / Yield strength
		0.002 [a] (lb./sq. in.)	2/3 E (lb./sq. in.)			Left end	Right end		
l₀	1 ×0.018	46,600	46,700	63,400	24.0	127	125	10.27×10⁶	[c]1.36
m₀	1 × .020	47,200	47,300	63,600	22.0	134	133	10.18	1.34
n₀	1 × .022	48,900	49,000	65,400	25.0	134	134	10.13	1.34
o₀	1 × .025	49,000	49,100	65,200	24.0	133	133	10.34	1.33
p₀	1 × .028	46,400	46,400	64,800	25.0	134	136	10.43	1.40
q₀	1 × .032	45,300	45,400	65,400	17.0	134	135	10.31	1.44
s₀	1 × .042	46,500	46,500	65,900	24.0	137	134	10.41	1.42
t₀	1 × .049	46,600	46,600	66,300	27.0	135	135	10.34	1.42
u₀	1 × .058	45,600	45,500	66,000	27.0	137	135	10.48	1.45
v₀	1 × .065	44,300	44,100	65,800	29.0	135	135	10.48	1.49
w₀	1 × .072	45,800	45,600	65,900	29.0	135	134	10.54	1.44
x₀	1 × .083	45,500	45,500	65,300	29.0	135	135	10.37	1.44
y₀	1 × .095	45,300	45,300	65,300	28.0	137	137	10.35	1.44
z₀	1 × .109	47,400	47,400	65,000	28.0	137	138	10.46	1.37
Aa₀	1 × .120	47,400	47,300	65,800	28.0	140	140	10.56	1.39
U₀	1½× .022	46,900	47,100	65,900	18.0	134	132	10.30	1.40
V₀	1½× .025	47,300	47,400	64,200	21.0	136	137	10.42	1.36
W₀	1½× .028	49,400	49,500	67,000	25.0	137	137	10.51	1.35
X₀	1½× .032	48,000	48,100	65,600	25.5	135	134	10.05	1.36
Y₀	1½× .035	50,200	50,300	66,200	27.0	142	142	10.40	1.32
Z₀	1½× .042	47,200	47,300	66,200	23.5	134	137	10.35	1.40
a₀	1½× .049	46,600	46,600	65,900	27.0	135	135	10.17	1.41
b₀	1½× .058	45,800	45,700	65,800	31.0	137	135	10.66	1.44
c₀	1½× .065	46,400	46,400	64,000	28.0	134	131	10.41	1.38
d₀	1½× .072	44,400	44,500	63,200	28.0	140	138	9.79	1.42
e₀	1½× .083	46,500	46,600	63,900	28.0	136	137	10.29	1.37
f₀	1½× .095	47,200	47,200	65,200	25.5	138	138	10.46	1.38
g₀	1½× .109	49,700	49,800	66,200	25.0	137	135	10.36	1.33
h₀	1½× .120	47,600	47,600	67,000	30.0	137	138	10.59	1.41
i₀	1½× .134	47,500	47,500	66,600	30.0	136	137	10.48	1.40
j₀	1½× .148	47,900	47,900	66,400	31.0	135	136	10.59	1.39
k₀	1½× .165	47,400	47,300	66,100	31.0	138	139	10.77	1.40
A₀	2 × .022	47,400	47,400	63,800	[d]16.5	133	132	10.48	1.35
B₀	2 × .025	49,400	49,400	62,800	[d]10.0	134	132	10.65	1.27
C₀	2 × .028	48,400	48,500	64,700	[d]11.0	134	134	10.49	1.33
D₀	2 × .032	48,300	48,400	64,500	23.0	132	131	10.38	1.33
E₀	2 × .035	48,900	49,000	65,400	24.0	134	131	10.50	1.33
F₀	2 × .042	49,600	49,500	64,100	23.0	135	132	10.75	1.30
G₀	2 × .049	50,000	49,900	65,200	22.5	134	133	10.75	1.31
I₀	2 × .065	46,100	46,000	65,100	30.0	134	131	10.61	1.42
J₀	2 × .072	48,600	48,700	66,200	27.0	136	133	10.32	1.36
K₀	2 × .083	47,400	47,200	66,000	29.0	134	134	10.81	1.40
L₀	2 × .095	47,900	47,800	65,100	30.0	133	133	10.73	1.36
M₀	2 × .109	49,700	49,800	65,100	29.0	133	134	10.40	1.31
N₀	2 × .120	46,700	46,700	65,800	29.0	134	133	10.53	1.41
O₀	2 × .134	47,100	47,100	64,000	28.0	133	131	10.56	1.36
P₀	2 × .148	48,000	48,000	66,000	28.0	133	134	10.29	1.38
Q₀	2 × .165	48,800	48,900	65,400	30.0	137	134	10.37	1.34
R₀	2 × .180	48,500	48,500	65,600	31.0	137	134	10.12	1.35
S₀	2 × .203	48,000	48,000	66,100	30.0	135	135	10.64	1.38
T₀	2 × .220	48,300	48,300	65,900	34.0	133	133	10.46	1.36
Average (51 speci-mens)		47,470	47,480	65,320	26.0	135	134	10.43	1.377

[a] Stress at which strain exceeds $\frac{stress}{10\times10^6}$ by 0.002 in./in.
[b] Vickers number for 10-kg weight.
[c] Based on 2/3 E yield strength.
[d] Broke at end of plug.

TABLE VII.—RESULTS OF TORSION TESTS OF CHROMIUM-MOLYBDENUM STEEL TUBES

| Specimen	Length L (in.)	Outside diameter D (in.)	Thickness t (in.)	L/D	t/D	Yield strength in shear by 5/9 G method (lb./sq. in.)	Mean fiber shear stress at failure (lb./sq. in.)	Shear modulus (lb./sq. in.)	Final type of failure [a]
A_1	19	0.750	0.0304	25.3	0.04055	48,600	50,600	11.55×10⁶	2 lobes.
A_2	19	.750	.0303	25.3	.04040	47,900	50,400	11.50	Do.
A_5	60	.751	.0302	79.9	.04020	49,500	51,100	12.05	Do.
B_1	19	1.001	.0381	19.0	.03807	54,900	57,000	11.55	Do.
B_2	19	1.001	.0380	19.0	.03795	56,000	57,300	11.80	Do.
B_3	19	1.001	.0380	19.0	.03795	57,400	57,700	11.36	Do.
C_1	19	1.128	.0479	16.9	.04245	54,300	56,400	11.80	Do.
C_2	19	1.127	.0480	16.9	.04255	54,400	56,700	11.86	Do.
C_6	60	1.127	.0480	53.2	.04255	54,500	57,700	11.86	Do.
D_1	19	1.503	.0580	12.6	.03860	59,800	61,500	11.75	Do.
D_2	19	1.503	.0580	12.6	.03860	59,700	61,800	11.75	Do.
D_3	19	1.503	.0581	12.6	.03866	58,000	61,400	11.97	Do.
D_4	19	1.503	.0581	12.6	.03866	59,000	60,800	11.70	Do.
D_5	48	1.503	.0581	31.9	.03866	58,500	59,800	11.52	Do.
E_1	19	2.004	.0652	9.5	.03255	6C,100	60,900	11.30	Do.
E_2	19	2.004	.0652	9.5	.03255	57,500	59,100	11.62	Do.
E_3	19	2.004	.0653	9.5	.03258	60,000	60,300	11.45	Do.
E_5	48	2.005	.0652	24.0	.03255	59,100	59,900	11.52	Do.
F_1	19	1.377	.0382	13.8	.02775	47,000	53,400	11.08	Do.
F_2	19	1.377	.0382	13.8	.02775	45,300	53,300	11.23	Do.
F_5	45	1.385	.0381	32.7	.02753	46,100	53,000	11.30	Do.
G_1	19	1.498	.0349	12.7	.02330	39,500	46,000	11.17	Do.
G_2	19	1.499	.0349	12.7	.02326	40,500	45,900	10.86	Do.
G_5	45	1.498	.0349	30.1	.02330	b47,200	43,800	11.83	Do.
H_1	19	1.510	.0528	12.6	.03500	b50,500	47,700	11.76	Do.
H_2	19	1.511	.0527	12.6	.03486	b49,800	47,400	11.42	Do.
I_1	19	1.510	.0685	12.6	.04540	b54,300	40,000	11.42	Do.
I_2	19	1.510	.0687	12.6	.04550	b52,200	38,000	11.42	Do.
J_1	19	1.503	.0845	12.6	.0562	b65,700	47,000	11.90	Do.
J_2	19	1.503	.0845	12.6	.0562	b65,500	47,100	11.83	Do.
J_5	47	1.503	.0845	31.4	.0562	b65,100	47,500	11.32	Do.
K_1	19	1.502	.0926	12.6	.0617	b68,600	63,500	11.90	Do.
K_2	19	1.503	.0925	12.6	.0616	b68,800	63,100	11.73	Do.
L_1	19	1.500	.1259	12.7	.0840	b62,900	54,500	12.00	Do.
L_2	19	1.499	.1258	12.7	.0840	b61,000	53,000	12.05	Do.
L_5	45	1.500	.1258	30.2	.0839	b59,400	51,500	11.30	Helix.
M_1	19	1.630	.0495	11.6	.03035	b55,800	54,500	11.55	2 lobes.
M_2	19	1.631	.0495	11.6	.03033	b57,400	54,500	11.72	Do.
N_1	19	1.753	.0509	10.8	.02905	b62,600	56,300	11.26	Do.
N_2	19	1.752	.0509	10.8	.02907	b61,700	57,000	11.26	Do.
N_5	45	1.752	.0507	26.1	.02895	b61,500	54,300	11.33	Do.
O_1	19	1.626	.0359	11.7	.02206	b54,600	54,500	11.60	Do.
O_2	19	1.625	.0358	11.7	.02202	55,400	------------	11.72	Do.
O_3	60	1.628	.0357	36.8	.02196	56,000	56,600	11.55	Do.
P_1	19	1.751	.0356	10.8	.02030	59,000	------------	11.62	Do.
P_2	19	1.752	.0354	10.8	.02022	57,900	------------	12.23	Do.
P_3	60	1.751	.0354	34.2	.02022	56,000	------------	11.65	Do.
Q_1	19	2.005	.0361	9.5	.01801	------------	56,400	11.30	Do.
Q_3	60	1.998	.0360	30.0	.01801	------------	53,100	11.10	Do.
R_1	19	1.124	.0316	16.9	.02815	b57,200	57,000	11.55	Do.
R_2	19	1.124	.0317	16.9	.02822	b59,100	58,900	11.83	Do.
R_3	60	1.124	.0317	53.4	.02822	------------	61,000	11.69	Do.
S_1	19	1.250	.0338	15.2	.02706	52,500	53,000	11.83	Do.
S_2	19	1.251	.0338	15.2	.02700	52,800	52,800	11.70	Do.
T_1	19	1.503	.0352	12.6	.02342	55,000	55,200	11.73	Do.
T_2	19	1.503	.0352	12.6	.02342	54,800	54,900	11.66	Do.
T_3	60	1.503	.0352	39.9	.02342	------------	52,900	11.60	Do.
U_1	19	1.506	.0501	12.6	.03339	59,000	61,700	11.76	Do.
U_2	19	1.506	.0501	12.6	.03330	59,100	61,600	11.50	Do.
U_3	60	1.506	.0501	39.8	.03330	59,600	61,900	11.80	Do.
V_1	19	2.500	.0341	7.6	.01364	41,100	41,300	11.16	Do.
V_2	19	2.506	.0336	7.6	.01340	40,500	40,500	10.80	Do.
V_3	60	2.504	.0340	24.0	.01358	------------	29,500	10.45	Do.
Average (63 specimens)						52,780	56,550	11.57	

[a] Type of failure as indicated by inspection of tube after removal from test fixture.
[b] Extrapolated value.

TABLE VIII.—RESULTS OF TORSION TESTS OF 17ST ALUMINUM-ALLOY TUBES

Specimen	Length L (in.)	Outside diameter D (in.)	Thickness t (in.)	L/D	t/D	Yield strength 2/3 G (lb./sq. in.)	Mean fiber shear stress at failure (lb./sq. in.)	Shear modulus (lb./sq. in.)	Final type of failure [a]
l_1	20	0.9997	0.0188	20.0	0.01880	------------	21,000	3.86×10^6	2 lobes.
l_2	60	1.0005	.0187	60.0	.01869	------------	19,400	3.86	Do.
m_1	20	.9994	.0199	20.0	.01991	21,900	21,900	3.89	Do.
m_2	60	1.0003	.0198	60.0	.01979	------------	20,500	3.89	Do.
n_1	20	1.0024	.0224	19.9	.02235	23,000	23,100	3.86	Do.
n_2	60	1.0021	.0224	59.8	.02235	------------	23,400	3.86	Do.
o_1	20	1.0016	.0252	19.9	.02516	23,000	23,400	3.88	Do.
o_2	60	1.0017	.0257	59.8	.02566	------------	25,200	3.88	Do.
p_1	20	1.0002	.0283	20.0	.02829	21,200	23,600	3.92	Do.
p_2	60	1.0006	.0285	60.0	.02848	22,600	24,200	4.00	Do.
q_1	20	1.0028	.0324	19.9	.03231	22,500	24,900	4.00	Do.
q_2	60	1.0024	.0325	59.8	.03242	23,500	26,000	3.92	Do.
s_1	20	1.0031	.0422	19.9	.04207	23,500	27,900	3.96	Do.
s_2	60	1.0018	.0423	59.8	.04222	24,800	29,200	4.08	Do.
t_1	20	1.0007	.0498	20.0	.04977	23,700	30,400	4.00	Do.
t_2	60	1.0013	.0498	59.9	.04974	24,600	31,300	4.05	Do.
u_1	20	1.0020	.0590	20.0	.05888	23,800	33,700	3.97	Do.
u_2	60	1.0027	.0588	59.8	.05864	24,100	33,700	3.97	Do.
v_1	20	1.0020	.0637	20.0	.06357	23,000	34,000	3.95	Do.
v_2	60	1.0024	.0637	59.8	.06355	24,300	35,200	3.94	Do.
w_1	20	1.0006	.0718	20.0	.07176	24,000	36,800	4.00	Do.
w_2	60	1.0004	.0717	60.0	.07167	25,400	38,600	4.00	Do.
x_1	20	.9994	.0832	20.0	.08325	23,600	40,000	3.97	Helix and 2 lobes.
x_2	60	.9998	.0832	60.0	.08322	25,000	41,200	3.97	Do.
y_1	20	.9975	.0938	20.0	.09403	23,700	41,400	3.97	Helix.
y_2	60	.9984	.0942	60.1	.09435	24,300	42,400	3.97	Helix and 2 lobes.
z_1	20	.9965	.1076	20.1	.10797	23,000	41,100	3.99	Helix.
z_2	60	.9971	.1074	60.2	.10771	24,000	41,900	3.99	Do.
Aa_1	20	1.0001	.1192	20.0	.11919	23,000	41,300	3.97	Do.
Aa_2	60	1.0005	.1188	60.0	.11874	24,100	42,400	3.97	Do.
U_1	20	1.4955	.0224	13.4	.01498	------------	20,100	3.96	2 lobes.
U_2	60	1.5000	.0227	40.0	.01513	------------	16,900	3.96	Do.
V_1	20	1.4996	.0244	13.3	.01627	------------	20,700	3.94	Do.
V_2	60	1.5003	.0244	40.0	.01626	------------	18,500	3.94	Do.
W_1	20	1.5066	.0285	13.3	.01892	------------	23,500	4.00	Do.
W_2	60	1.5055	.0285	39.9	.01893	------------	22,000	3.94	Do.
X_1	20	1.5035	.0330	13.3	.02195	22,800	23,600	3.96	Do.
X_2	60	1.5033	.0330	39.9	.02195	22,200	22,800	3.96	Do.
Y_1	20	1.4997	.0354	13.3	.02360	23,500	24,400	3.97	Do.
Y_2	60	1.5018	.0354	39.9	.02357	------------	24,800	3.97	Do.
Z_1	20	1.5017	.0436	13.3	.02903	22,500	25,100	3.88	Do.
Z_2	60	1.5022	.0435	39.9	.02896	23,100	24,100	3.93	Do.
a_1	20	1.5001	.0491	13.3	.03273	23,000	26,400	3.92	Do.
a_2	60	1.5006	.0497	40.0	.03312	23,600	26,100	3.97	Do.
b_1	20	1.5031	.0585	13.3	.03892	23,600	27,000	3.94	Do.
b_2	60	1.5035	.0585	39.9	.03891	24,200	27,700	3.94	Do.
c_1	20	1.4995	.0634	13.3	.04228	22,100	27,700	3.95	Do.
c_2	60	1.5000	.0636	40.0	.04240	22,600	27,400	3.97	Do.
d_1	20	1.4988	.0719	13.4	.04797	22,500	29,600	3.97	Do.
d_2	60	1.4980	.0721	40.1	.04813	23,200	30,500	3.99	Do.
e_1	20	1.5002	.0837	13.3	.05579	22,000	31,900	3.94	Do.
e_2	60	1.5007	.0837	40.0	.05577	22,900	31,700	3.98	Do.
f_1	20	1.5019	.0956	13.3	.06365	22,400	33,900	3.93	Do.
f_2	60	1.5015	.0955	39.9	.06360	23,000	34,000	3.93	Do.
g_1	20	1.5004	.1107	13.3	.07378	24,000	39,300	3.95	Do.
g_2	60	1.4996	.1107	40.0	.07382	24,600	37,700	3.97	Helix and 2 lobes.
h_1	20	1.4988	.1192	13.4	.07953	23,300	40,600	4.02	2 lobes.
h_2	60	1.4992	.1195	40.0	.07971	23,400	40,600	4.00	Helix and 2 lobes.
i_1	20	1.5020	.1337	13.3	.08901	23,500	42,900	3.97	Do.
i_2	60	1.5014	.1337	39.9	.08905	23,700	41,900	4.00	Do.
j_1	20	1.4991	.1461	13.3	.09746	23,500	42,700	3.96	Fracture—slight helix.
j_2	60	1.4997	.1466	40.0	.09775	23,800	42,800	3.98	Helix.
k_1	20	1.5010	.1658	13.3	.11046	23,000	42,700	3.97	Do.
k_2	60	1.5010	.1659	39.9	.11053	22,900	41,500	3.93	Do.
A_1	20	2.0035	.0202	10.0	.01008	------------	16,000	3.86	2 lobes.
A_2	60	2.0029	.0202	30.0	.01009	------------	12,200	3.86	Do.
B_1	20	2.0058	.0255	10.0	.01271	------------	19,700	3.95	Do.
B_2	60	2.0037	.0254	30.0	.01268	------------	15,000	3.95	Do.
C_1	20	2.0047	.0274	10.0	.01367	------------	21,200	3.97	Do.
C_2	60	2.0048	.0274	29.9	.01367	------------	16,500	3.97	Do.
D_1	20	2.0061	.0314	10.0	.01565	------------	21,800	3.95	Do.
D_2	60	2.0044	.0315	29.9	.01572	------------	19,000	3.95	Do.
E_1	20	2.0054	.0359	10.0	.01790	23,300	23,300	3.95	Do.
E_2	60	2.0033	.0361	29.9	.01802	------------	20,200	3.95	Do.
F_1	20	2.0020	.0426	10.0	.02128	23,700	24,600	3.99	Do.
F_2	60	2.0020	.0426	29.9	.02128	------------	23,200	3.99	Do.
G_1	20	2.0053	.0509	10.0	.02538	23,800	25,100	3.97	Do.
G_2	60	2.0035	.0510	29.9	.02546	24,600	24,700	3.97	Do.
I_1	20	2.0010	.0668	10.0	.03338	22,900	26,100	3.92	Do.
I_2	60	1.9998	.0670	30.0	.03350	23,300	25,700	3.92	Do.
J_1	20	1.9988	.0716	10.0	.03582	22,600	26,900	3.95	Do.
J_2	60	1.9988	.0716	30.0	.03582	23,000	27,000	3.95	Do.
K_1	20	2.0012	.0833	10.0	.04162	22,700	28,100	3.97	Do.
K_2	60	2.0013	.0838	30.0	.04187	22,800	27,700	3.97	Do.
L_1	20	2.0012	.0952	10.0	.04757	23,200	30,700	3.98	Do.
L_2	60	2.0009	.0952	30.0	.04758	23,300	29,500	3.98	Do.
M_1	20	2.0002	.1110	10.0	.05549	24,700	33,900	3.97	Do.
M_2	60	1.9988	.1109	30.0	.05548	24,600	33,200	3.97	Do.
N_1	20	2.0027	.1206	10.0	.06022	22,500	35,000	4.01	Do.
N_2	60	2.0026	.1209	29.9	.06037	22,500	34,400	4.01	Do.
O_1	20	1.9952	.1316	10.0	.06596	22,400	36,700	3.96	Do.
O_2	60	1.9988	.1326	30.0	.06634	22,500	34,700	3.96	Do.
P_1	20	2.0027	.1487	10.0	.07425	24,000	40,200	3.99	Helix and 2 lobes.
P_2	60	2.0027	.1496	29.9	.07470	24,000	39,600	3.99	Helix.
Q_1	20	1.9974	.1662	10.0	.08321	23,500	41,600	3.97	2 lobes.
Q_2	60	1.9971	.1654	30.0	.08282	23,300	40,300	3.97	Helix.
R_1	20	1.9980	.1816	10.0	.09089	22,500	42,200	3.99	2 lobes.
R_2	60	1.9978	.1816	30.0	.09090	22,500	41,500	3.99	Helix and 2 lobes.
S_1	20	2.0018	.2039	10.0	.10186	22,600	41,400	3.97	Fracture, slight helix.
S_2	60	2.0027	.2040	29.9	.10186	22,400	42,200	3.97	Helix.
T_1	20	1.9994	.2196	10.0	.10983	23,500	43,000	4.00	Fracture.
T_2	60	1.9989	.2206	30.0	.11036	23,400	42,400	4.00	Helix.
Average (102 specimens)						23,310	30,380	3.96	

[a] Type of failure as indicated by inspection of tube after removal from test fixture.
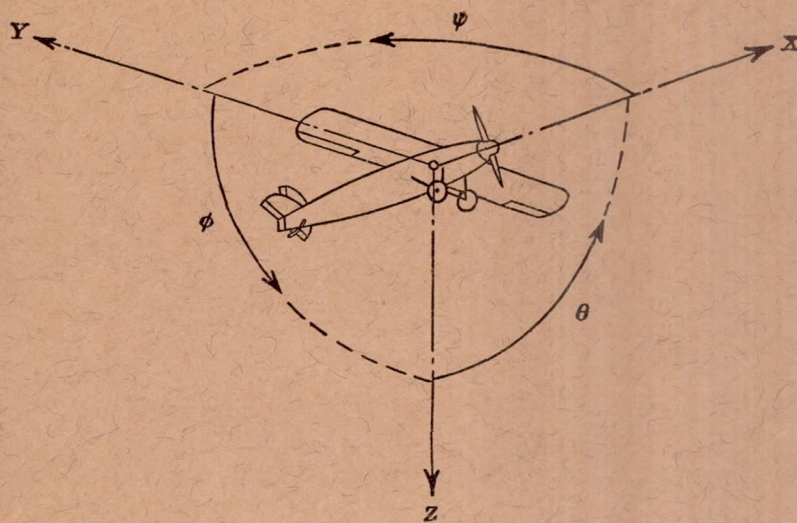
Positive directions of axes and angles (forces and moments) are shown by arrows

Axis		Force (parallel to axis) symbol	Moment about axis			Angle		Velocities	
Designation	Symbol		Designation	Symbol	Positive direction	Designation	Symbol	Linear (component along axis)	Angular
Longitudinal	X	X	Rolling	L	$Y \longrightarrow Z$	Roll	ϕ	u	p
Lateral	Y	Y	Pitching	M	$Z \longrightarrow X$	Pitch	θ	v	q
Normal	Z	Z	Yawing	N	$X \longrightarrow Y$	Yaw	ψ	w	r

Absolute coefficients of moment

$$C_l = \frac{L}{qbS} \qquad C_m = \frac{M}{qcS} \qquad C_n = \frac{N}{qbS}$$
(rolling) (pitching) (yawing)

Angle of set of control surface (relative to neutral position), δ. (Indicate surface by proper subscript.)

4. PROPELLER SYMBOLS

D, Diameter

p, Geometric pitch

p/D, Pitch ratio

V', Inflow velocity

V_s, Slipstream velocity

T, Thrust, absolute coefficient $C_T = \dfrac{T}{\rho n^2 D^4}$

Q, Torque, absolute coefficient $C_Q = \dfrac{Q}{\rho n^2 D^5}$

P, Power, absolute coefficient $C_P = \dfrac{P}{\rho n^3 D^5}$

C_s, Speed-power coefficient $= \sqrt[5]{\dfrac{\rho V^5}{P n^2}}$

η, Efficiency

n, Revolutions per second, r.p.s.

Φ, Effective helix angle $= \tan^{-1}\left(\dfrac{V}{2\pi rn}\right)$

5. NUMERICAL RELATIONS

1 hp. $= 76.04$ kg-m/s $= 550$ ft-lb./sec.

1 metric horsepower $= 1.0132$ hp.

1 m.p.h. $= 0.4470$ m.p.s.

1 m.p.s. $= 2.2369$ m.p.h.

1 lb. $= 0.4536$ kg.

1 kg $= 2.2046$ lb.

1 mi. $= 1,609.35$ m $= 5,280$ ft.

1 m $= 3.2808$ ft.